Constraints on the sum of the neutrino masses in dynamical dark energy models with $w(z) \geq -1$ are tighter than those obtained in ΛCDM

Sunny Vagnozzi,[1,2,*] Suhail Dhawan,[1] Martina Gerbino,[1] Katherine Freese,[1,2,3] Ariel Goobar,[1] and Olga Mena[4]

[1]*The Oskar Klein Centre for Cosmoparticle Physics, Department of Physics, Stockholm University, SE-106 91 Stockholm, Sweden*

[2]*The Nordic Institute for Theoretical Physics (NORDITA), Roslagstullsbacken 23, SE-106 91 Stockholm, Sweden*

[3]*Leinweber Center for Theoretical Physics, Department of Physics, University of Michigan, Ann Arbor, Michigan 48109, USA*

[4]*Instituto de Física Corpuscular (IFIC), Universidad de Valencia-CSIC, E-46980, Valencia, Spain*

(Received 1 February 2018; published 1 October 2018)

We explore cosmological constraints on the sum of the three active neutrino masses M_ν in the context of dynamical dark energy (DDE) models with equation of state (EoS) parametrized as a function of redshift z by $w(z) = w_0 + w_a z/(1+z)$, and satisfying $w(z) \geq -1$ for all z. We make use of cosmic microwave background data from the Planck satellite, baryon acoustic oscillation measurements, and supernovae Ia luminosity distance measurements, and perform a Bayesian analysis. We show that, within these models, the bounds on M_ν *do not degrade* with respect to those obtained in the ΛCDM case; in fact, the bounds are slightly tighter, despite the enlarged parameter space. We explain our results based on the observation that, for fixed choices of w_0, w_a such that $w(z) \geq -1$ (but not $w = -1$ for all z), the upper limit on M_ν is tighter than the ΛCDM limit because of the well-known degeneracy between w and M_ν. The Bayesian analysis we have carried out then integrates over the possible values of w_0-w_a such that $w(z) \geq -1$, all of which correspond to tighter limits on M_ν than the ΛCDM limit. We find a 95% credible interval (C.I.) upper bound of $M_\nu < 0.13$ eV. This bound can be compared with the 95% C.I. upper bounds of $M_\nu < 0.16$ eV, obtained within the ΛCDM model, and $M_\nu < 0.41$ eV, obtained in a DDE model with arbitrary EoS (which allows values of $w < -1$). Contrary to the results derived for DDE models with arbitrary EoS, we find that a dark energy component with $w(z) \geq -1$ is unable to alleviate the tension between high-redshift observables and direct measurements of the Hubble constant H_0. Finally, in light of the results of this analysis, we also discuss the implications for DDE models of a possible determination of the neutrino mass ordering by laboratory searches.

DOI: 10.1103/PhysRevD.98.083501

I. INTRODUCTION

The nature of the dark energy (DE) driving the accelerated expansion of the Universe remains one of the greatest open problems in cosmology [1–19]. The most economical DE candidate is a cosmological constant (CC) related to vacuum energy density. The equation of state (EoS) of such a component is $w_{\rm DE} = P_{\rm DE}/\rho_{\rm DE} = -1$, where $P_{\rm DE}$ and $\rho_{\rm DE}$ are the pressure and energy density of the DE, respectively. The CC model is, however, at odds with theoretical expectations of the magnitude of the CC, an issue dubbed the *cosmological constant problem* [20–23]. An alternative solution to this issue posits the existence of a dynamical dark energy (DDE) component [24–26], which implies a redshift-dependent equation of state $w(z)$.

The value $w = -1$ plays an important role from the theoretical point of view, as it demarcates two very different physical regimes [27–37]. The energy density of a component with $w < -1$ increases with time as the Universe expands. More importantly, such a component would violate the dominant energy condition, which imposes the inequality $|P| \leq \rho$ [38].[1] A component with EoS $w < -1$ is usually referred to as "phantom energy". It has been shown that a universe dominated by a phantom DE component would end in a big rip: the dissociation of any bound system due to the DE energy density becoming

*sunny.vagnozzi@fysik.su.se

[1]We note that this issue can be avoided in models in which the effective dark energy component appears to violate the dominant energy condition while the full theory does not (e.g., [37]).

infinite in a finite amount of time [39].[2] Examples of nonphantom dark energy models include many quintessence models [55–58] and Cardassian cosmology [59–61].

Recent works have studied and forecasted cosmological constraints on the sum of the three active neutrino masses, $M_\nu = \sum_i m_i$ (where m_i are the masses of the individual mass eigenstates), within the context of the standard cosmological model, the ΛCDM model, which fixes $w = -1$ [4,5,62–96]. The exact figures vary slightly depending on the data sets used, but combinations of some of the most recent and reliable data sets are converging toward a robust 95% credible interval (C.I.) upper bound of $M_\nu \lesssim 0.15$ eV within the ΛCDM model.

It is the goal of this paper to reconsider these bounds if one retreats from the restricted value of $w = -1$ assumed by ΛCDM. In our work we consider dynamical dark energy with monotonic redshift dependence $w(z)$ given by the standard Chevallier-Polarski-Linder (CPL) parametrization in Eq. (1) [97,98]. We use a combination of some of the most recent and robust data sets, which include cosmic microwave background (CMB) measurements from the Planck satellite, baryon acoustic oscillation (BAO) measurements from the SDSS and 6dFGS surveys, and supernovae Type-Ia (SNeIa) luminosity distance measurements from the JLA catalogue.

One might worry that the neutrino mass bounds could weaken dramatically if the parameter space is enlarged to allow for values of the equation of state other than $w = -1$. Indeed, recent work showed that the cosmological bounds on M_ν are weaker when one enlarges the parameter space to other values of $w(z)$ including phantom values $w < -1$. In fact, there exists a well-known degeneracy between the DE EoS w and the sum of the three active neutrino masses M_ν [66,99–114]. However, the main result of our paper is that the cosmological bounds on neutrino masses, in fact, become more restrictive for the case of a DE component with $w(z) \geq -1$ than for the standard ΛCDM case of $w = -1$. A comprehensive explanation for this effect will be provided.

From neutrino oscillation data, we know that at least two out of the three neutrino mass eigenstates m_i should be massive, as two different mass splittings between the three active neutrinos are measured. We also know that the smallest mass splitting governs solar neutrino transitions and that it is positive. However, current data are not able to determine the sign of the largest mass splitting, which governs atmospheric neutrino transitions. Therefore, we are left with two possibilities: either the largest mass splitting is positive [normal ordering (NO)] or it is negative [inverted ordering (IO)]. Neutrino oscillation data are currently unable to distinguish between the two possible scenarios. Nevertheless, they impose a lower limit to M_ν of $M_{\nu,\mathrm{min}} \simeq 0.1$ eV within IO and $M_{\nu,\mathrm{min}} \simeq 0.06$ eV within NO [74,76,115–122].

If one performs a Bayesian analysis, then we find that our bounds imply a mild preference for NO due to parameter space volume effects. Indeed, the available mass range is larger for NO because it goes all the way down to $M_\nu \simeq 0.06$ eV rather than only down to $M_\nu \simeq 0.1$ eV for IO. We quantify this preference in terms of probability odds that we compute following Refs. [66,123]. If future laboratory experiments determine the mass ordering to be inverted, and if we exclude nonstandard physics in either the neutrino or the gravitational sector, one could conclude that the current accelerated expansion of the Universe is likely driven by a component with $w(z) < -1$ within DDE models.

The paper is structured as follows: in Sec. II, we introduce the parametrization adopted for the DDE component, and the conditions imposed on the parameters of the DDE model to satisfy $w(z) \geq -1$; in Sec. III, we present the statistical approach and the data set employed in this analysis. We discuss the results of this analysis in Sec. IV and we finally conclude in Sec. V. For the busy reader who wants to skip to the main results, a summary of the bounds obtained is available in Table I, and useful visual representations of the same results are also provided in Figs. 1 and 4.

II. DYNAMICAL DARK ENERGY PARAMETRIZATIONS

The simplest parametrization of a DDE component is the CPL parametrization [97,98]. In CPL models, the EoS w is parametrized as a function of redshift z as

$$w_{\mathrm{DDE}}(z) = w_0 + w_{\mathrm{a}} \frac{z}{1+z}, \tag{1}$$

where $w_0 = w_{\mathrm{DDE}}(z=0)$ denotes the DE EoS at the present time. This equation corresponds to the first two terms in a Taylor expansion of the EoS in powers of the scale factor $a = 1/(1+z)$, around the present time. The truncated expansion of Eq. (1) is appropriate if the DE EoS is sufficiently smooth and does not oscillate in cosmic time.[3]

It follows from Eq. (1) that the nonphantom (NP) $[w(z) \geq -1]$ condition can be satisfied by imposing the following hard priors:

[2] A notable exception is found in the case when $w(z) \to -1$ asymptotically in the future (that is, where the future geometry is asymptotically de Sitter) [40]. This occurs, for instance, in bimetric gravity [41–44] as well as in other modified gravity theories (see, e.g., [45–49]) or more complex dark energy scenarios [50–54].

[3] For models where the DE EoS oscillates, different parametrizations are required, such as those proposed in Refs. [124–126] or used in recent observational studies [127–129]. It is beyond the scope of this work to extend our considerations on the neutrino mass bounds to these types of DE models.

$$w_0 \geq -1, \qquad w_0 + w_a \geq -1(\mathrm{NP}). \tag{2}$$

The first prior imposes the nonphantom condition at present time ($z = 0$). The second prior imposes the same condition in the far past, since $\lim_{z\to\infty} w_{\mathrm{DDE}}(z) = w_0 + w_a$. The EoS in Eq. (1) is monotonic. Therefore, it is sufficient to impose the NP condition both at the present time and in the far past for the NP condition to hold throughout the Universe expansion history.

The energy density of a dark energy component corresponding to Eq. (1) takes the form

$$\Omega_{\mathrm{DE}}(z) = \Omega_{\mathrm{DE},0}(1+z)^{3(1+w_0+w_a)} \exp\left(-3w_a \frac{z}{1+z}\right), \tag{3}$$

where $\Omega_{\mathrm{DE},0}$ is the current dark energy density. The DE component dominates over the other components for $0 < z \lesssim z_{m\mathrm{DE}}$, with $z_{m\mathrm{DE}} \approx 0.3$ the redshift of matter-dark energy equality. In this range of redshifts, the energy density of a nonphantom dynamical dark energy model with $w(z) \geq -1$ is always greater than that of a corresponding CC model with the same $\Omega_{\mathrm{DE},0}$.

A wide class of smooth nonphantom dynamical dark energy models can be probed if we make use of the EoS given by Eq. (1) and we impose the priors in Eq. (2). We shall refer to this class of models with the acronym *NPDDE* (*nonphantom dynamical dark energy*). Let us emphasize that the priors in Eq. (2) are *crucial* in the derivation of the results we obtain. These priors ensure the stability of the dark energy component and differ from priors considered in previous analyses in the literature [130–138].

III. DATA SETS AND ANALYSIS METHODOLOGY

We compute constraints on the sum of the three active neutrino masses M_ν with a combination of the most recent cosmological data sets. We consider measurements of the CMB temperature anisotropies (TT) from the Planck 2015 data release [139]. We impose a Gaussian prior on the optical depth to reionization of $\tau = 0.055 \pm 0.009$ as a proxy for measurements of CMB polarization at large scales from the upcoming Planck 2018 release. This prior choice is motivated by the 2016 Planck reanalyses of low-resolution maps in polarization from the Planck High Frequency Instrument [140]. In addition to CMB measurements, we consider BAO measurements from the following catalogues: the SDSS-III BOSS DR11 CMASS and LOWZ galaxy samples [141], the DR7 Main Galaxy Sample (MGS) [142], and the 6dFGS survey [143]. We also include SNeIa luminosity distance measurements from the SDSS-II/SNLS3 Joint Light-Curve Analysis (JLA) catalogue [144–146]. We refer to the combination of the CMB TT, τ prior, BAO, and SNeIa data sets as "base."

We also consider the inclusion of CMB polarization and temperature-polarization spectra (TE, EE) at small scales ($\ell > 30$) from the Planck 2015 data release [139] to the baseline data set. We refer to the combination of the CMB TT, TE, EE, τ prior, BAO, and SNeIa data sets as "pol."

The cosmological model is described by the usual six parameters of the ΛCDM model: the baryon and cold dark matter physical energy densities $\Omega_\mathrm{b}h^2$ and $\Omega_\mathrm{c}h^2$, the angular scale of the acoustic horizon at decoupling Θ_s, the optical depth to reionization τ, as well as the amplitude and tilt of the primordial power spectrum A_s and n_s. To this set of parameters, we add the DE EoS parameters w_0 and w_a, and the sum of the three active neutrino masses M_ν. We make use of the publicly available Markov chain Monte Carlo (MCMC) package CosmoMC [147] to efficiently sample the parameter space.

The treatment of M_ν deserves a further comment. First, we assume three massive degenerate neutrinos, i.e., three massive eigenstates with equal mass $M_\nu/3$. This assumption is a valid approximation of the true neutrino mass spectrum, given the current sensitivity of cosmological data [73,107,148].

Next, we impose a top-hat prior of $M_\nu \geq 0$ eV. For the purposes of obtaining bounds on neutrino mass from cosmology, we ignore the lower limit $M_{\nu,\mathrm{min}} \simeq 0.06$ eV set by neutrino oscillation experiments.[4] We believe this choice is appropriate for the purpose of this work, because it ensures a bound on M_ν relying exclusively on cosmological data. For recent works discussing different choices of prior on M_ν, see, for instance, Refs. [150–157].

Moreover, it is fair to say that the only truly *a priori* information about M_ν is its positivity, i.e., $M_\nu \geq 0$ eV. The fact that $M_\nu \geq 0.06$ eV coming from oscillation experiments is not *a priori* but, in fact, *a posteriori* of the oscillation experiments. While the fact that $M_\nu \geq 0.06$ eV can be incorporated as a prior, it is perhaps formally more correct to include it as an external oscillations likelihood.[5] When viewed from this perspective, it is absolutely clear how our choice of adopting the prior $M_\nu \geq 0$ eV is actually independent of the choice of relying exclusively on

[4]We note that the prior $M_\nu \geq 0$ eV is in principle improper since it is unconstrained for $M_\nu \to \infty$ (see [149] for details about proper priors in the astronomy literature). In practice, we adopt a cutoff at $M_{\nu,\mathrm{max}} = 3$ eV, which makes our prior proper for all intents and purposes. This choice ensures that a large region of the parameter space is sampled, including regions where we already expect the posterior probability to be vanishing from previous experiments (i.e., the region $M_\nu \gg 1$ eV). These unlikely regions of the parameter space are, in fact, quickly discarded by the MCMC sampling algorithm, and only the region of highest posterior probability density is effectively sampled. For the purposes of our analysis, this is equivalent to taking the limit $M_{\nu,\mathrm{max}} \to \infty$, making our proper prior *de facto* a proxy for the improper prior we describe above. Our result is unaffected by any other choice of a sufficiently high value of $M_{\nu,\mathrm{max}}$, as long as the posterior probability density for $M_\nu > M_{\nu,\mathrm{max}}$ is known to be vanishingly small (from previous experiments, analytical considerations, or any other argument).

[5]We thank the referee for bringing this argument to our attention in a very clear way.

cosmological data, but rather reflects the only genuine *a priori* information really present in the problem. The choice of relying exclusively on cosmological data is instead reflected in our choice of not including the oscillations likelihood. Nonetheless, in Appendix A, we briefly discuss the impact including oscillation data. We find that including the oscillations likelihood (in the approximate, but still appropriate to zeroth order, form we choose) has no impact on the conclusions of our work. We further note that for all intents and purposes, as far as upper limits on M_ν (which are the subject of this work) are concerned, the oscillations likelihood can be to zeroth approximation included as a sharp cutoff at $M_\nu = 0.06$ eV, because the uncertainty to which $M_{\nu,\mathrm{min}} \simeq 0.06$ eV is subject is extremely tiny (but an uncertainty is nonetheless present, whereas the physical lower bound $M_\nu \geq 0$ eV is instead subject to no uncertainty).

In any case, we believe that the approach adopted in this work also allows for a consistency check of the underlying cosmological model. Suppose that we assume a certain cosmological model, and then obtain a cosmological bound on M_ν which lies significantly below ~0.06 eV. Such a cosmological bound would indicate that either the cosmological model in question is in tension with results from oscillation experiments or that nonstandard neutrino physics is required. For example, models with nonstandard neutrino interactions leading to a vanishing neutrino energy density today have been proposed [158]. In these cases, the cutoff of the M_ν prior at $M_\nu = 0$ eV can be viewed as a phenomenological proxy of the effect of a lower energy density of neutrinos with respect to the limits imposed by neutrino oscillation measurements. Note that we are implicitly excluding the possibility that such a finding could be a signal for unaccounted systematics in the data set employed.

Finally, we combine results from cosmology and neutrino oscillation experiments to quantify the preference for one of the two neutrino mass orderings. In this part of the work, we do impose lower bounds on neutrino mass from oscillation experiments, although we previously did not use them in obtaining bounds on neutrino masses. We follow the Bayesian approach illustrated in [66,123]. We denote by $\pi(I)$, $\pi(N)$ the *prior probabilities* for the normal and inverted ordering, respectively. Then, we compute p_O (where $O = N, I$), the *posterior probabilities* for each of the two orderings, as follows:

$$p_O = \frac{\pi(O)\int_0^\infty dm_0 \mathcal{L}(D|m_0, O)}{\pi(N)\int_0^\infty dm_0 \mathcal{L}(D|m_0, N) + \pi(I)\int_0^\infty dm_0 \mathcal{L}(D|m_0, I)}. \tag{4}$$

In Eq. (4), m_0 is the mass of the lightest neutrino eigenstate and $\mathcal{L}(D|m_0, O)$ is the likelihood of cosmological data D. The above Eq. (4) implicitly assumes a cutoff $m_{0,\mathrm{max}} \to \infty$ in the prior probability for m_0. Moreover, $m_{0,\mathrm{max}}$ should take the same value for both orderings and be large enough so as not to cut the prior in a region where the posterior would otherwise be significantly different from zero (so that it is effectively the data through the likelihood, rather than the prior itself, which cuts the region of high m_0; see footnote 4 for a previous related discussion when considering the formally improper prior on M_ν). In this way, both the numerator and the denominator should formally contain a $1/m_{0,\mathrm{max}}$ normalization factor, which then cancels out when taking the ratio appearing in Eq. (4). We take $\mathcal{L}(D|m_0, O)$ from the analysis of cosmological data illustrated in this work. We use the values of $\pi(I)$, $\pi(N)$ from the global Bayesian analysis of neutrino oscillation measurements [117]. For further details about how to compute $\mathcal{L}(D|m_0, O)$ and get to Eq. (4), we refer the reader to the thorough discussions in [66,123]. We convey the results in terms of probability odds of normal versus inverted ordering ($p_{\mathrm{NO}} : p_{\mathrm{IO}}$).

We follow the approach of [66,123] as it is a quick, yet reliable, way to quantify the preference for the normal ordering in different cosmological scenarios. The method used in this work should be kept in mind when one compares the results quoted here with results from other works. Indeed, we remind the reader that alternative approaches can be adopted to quantify the statistical preference for the neutrino mass ordering [74,150,159]. For the sake of comparison, in Appendix B we report an alternative estimate of the sensitivity to the mass ordering based on the Akaike information criterion (AIC). The specific outcomes of each analysis should be interpreted only in light of the method adopted.

IV. RESULTS

In this section, we present the bounds on the sum of the three active neutrino masses; we provide a thorough physical explanation of the results; we discuss the Bayesian statistical approach we have used, as well as the dependence of our results on this approach; and we conclude by commenting on the implications of our results for the determination of the neutrino mass ordering.

A. Bounds on neutrino masses

Table I shows the bounds on the sum of the neutrino masses M_ν for three cases: (a) a dark energy component satisfying the dominant energy condition, with EoS $w(z) \geq -1$ throughout the expansion history of the Universe [nonphantom dynamical dark energy (NPDDE)]; (b) the standard cosmological model (ΛCDM) with cold dark matter and a cosmological constant where $w(z) = -1$ is fixed; (c) a generic DDE model with EoS given by the CPL parametrization, Eq. (1), with w_0 and w_a free to vary even within the phantom region where $w(z) < -1$. We refer to this last model as $w_0 w_a$CDM. Constraints on M_ν are presented for the two different combinations of cosmological data sets, base and pol, described at the beginning of Sec. III.

TABLE I. The 95% C.I. upper bounds on the sum of the neutrino masses M_ν. Columns correspond to the different cosmological models assumed in this work: (a) a dark energy component satisfying the dominant energy condition, with EoS parametrized through Eq. (1) and satisfying $w(z) \geq -1$ throughout the expansion history of the Universe (NPDDE); (b) the standard cosmological model (ΛCDM) with cold dark matter and a cosmological constant where $w(z) = -1$ is fixed; (c) a generic DDE model with EoS given by the CPL parametrization, Eq. (1), with w_0 and w_a free to vary even within the phantom region where $w(z) < -1$ ($w_0 w_a$CDM). Rows report the constraints on M_ν for two different combinations of cosmological data sets, base and pol. These two combinations include CMB, BAO, and SNeIa data, and they only differ in the use of CMB polarization data at small scales, as described in the text at the beginning of Sec. III.

	$w(z) \geq -1$(NPDDE)	$w(z) = -1$(ΛCDM)	$w_0 w_a$CDM
Data set: base	$M_\nu < 0.13$ eV	$M_\nu < 0.16$ eV	$M_\nu < 0.41$ eV
Data set: pol	$M_\nu < 0.11$ eV	$M_\nu < 0.13$ eV	$M_\nu < 0.37$ eV

For the ΛCDM model, we find 95% C.I. upper bounds of $M_\nu < 0.16$ eV for the base data set and $M_\nu < 0.13$ eV for the pol data set. When we instead assume the more generic $w_0 w_a$CDM model that also allows for $w(z) < -1$, the 95% C.I. upper bound on M_ν is significantly relaxed to $M_\nu < 0.41$ eV for the base data set and $M_\nu < 0.37$ eV for the pol data set. These broader bounds are expected, given the well known degeneracy between M_ν and an arbitrary DDE component.

We now consider a NPDDE model and impose $w(z) \geq -1$ throughout the expansion history. In this case, we find the stringent 95% C.I. upper bounds of $M_\nu < 0.13$ eV for the base data set and $M_\nu < 0.11$ eV for the pol data set.

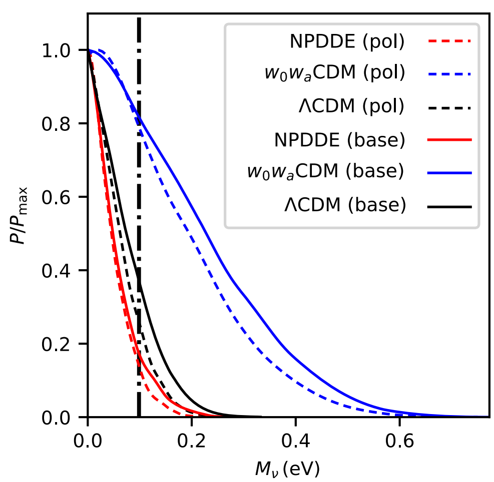

FIG. 1. One-dimensional posterior probabilities of the sum of the three active neutrino masses M_ν (in eV) for three cases: the $w_0 w_a$CDM generic DDE case which allows for values of w both smaller than or larger than -1 (in blue lines), the ΛCDM case (in black lines), and the NPDDE model with $w(z) \geq -1$ (in red lines). Results have been obtained using a Bayesian analysis that marginalizes over all applicable w_0, w_a values, and are shown for the two data set combinations employed in this work as described at the beginning of Sec. III: solid lines for base (using CMB, BAO, and SN data), dashed lines for pol (also including CMB polarization at small scales). The vertical black dot-dashed line corresponds to the minimal mass of $M_{\nu,\rm min} \approx 0.1$ eV allowed by neutrino oscillation data within the inverted ordering.

Therefore, we find that *the constraints on the sum of the neutrino masses in dynamical dark energy models with $w(z) \geq -1$ are slightly tighter than those obtained in* ΛCDM, despite the enlarged parameter space (two extra parameters) in NPDDE models. We note that the upper bounds found within the NPDDE model are also very close to the minimal mass allowed in the inverted ordering scenario, $M_{\nu,\rm min} \simeq 0.1$ eV.

Figure 1 depicts the one-dimensional posterior probabilities of M_ν for the $w_0 w_a$CDM generic DDE case (in blue lines), the ΛCDM case (in black lines), and the NPDDE model with $w(z) \geq -1$ (in red lines). Results for the two data set combinations employed in this work are shown: solid lines for base, dashed lines for pol. For each data set combination, the significant shift of the upper bounds on M_ν to smaller values is visually clear as one moves from the blue to the red curves. The vertical black dot-dashed line corresponds to the minimal mass of $M_{\nu,\rm min} \approx 0.1$ eV allowed by neutrino oscillation data within the inverted ordering.

B. Physical explanation of results

We have observed that the bounds on M_ν in the NPDDE model are not weaker—and actually slightly tighter—than those in ΛCDM. Here we provide the physical explanation for these results. The reader can refer to Refs. [101–107] for comprehensive reviews of the effects of massive neutrinos in cosmology.[6]

[6]Modifying the assumed expansionary history of the Universe will generically lead to different conclusions concerning M_ν. The reason is that the effect of M_ν on cosmological data is degenerate with other parameters governing the expansionary history, such as the DE EoS w: in other words, the effect on cosmological observables of a change in M_ν (for instance, the resulting change in the distance to last scattering, further discussed later in this section) can be compensated by adjusting these other parameters. Therefore, an expansionary history which is different from ΛCDM leads to bounds on M_ν which are different from those obtained assuming ΛCDM. Obviously, the same is true if the expansionary history is restricted to a class of models of which ΛCDM represents a particular case: in our case, ΛCDM represents the particular case of the NPDDE class of models, when $w_0 = -1$ and $w_a = 0$.

The CMB temperature data accurately constrain the position and amplitude of the first acoustic peak in the CMB power spectrum. These constraints entail a very precise determination of the angular size of the sound horizon at decoupling Θ_s and of the redshift of matter-radiation equality z_{eq}. Therefore, any change in the DE sector should be compensated by shifts in the other cosmological parameters such that Θ_s and z_{eq} remain approximately fixed.

The angular size of the first peak Θ_s is defined as the ratio between the sound horizon at decoupling r_s and the angular diameter distance to last scattering D_A. The sound horizon at decoupling r_s is essentially fixed by pre-recombination physics. It is thus unaffected by changes in the dark energy sector, which are only relevant at late times. The angular diameter distance to last scattering D_A is instead sensitive to the late-time evolution of the Universe. Therefore, D_A is affected by the physics of dark energy.

In order to keep Θ_s unchanged in the NPDDE framework, it is necessary that D_A remains fixed as well. Up to proportionality factors, D_A is given by

$$D_A(z_{\rm LS}) \propto \frac{1}{H_0}\int_0^{z_{\rm LS}} \frac{dz}{E(z)}, \qquad (5)$$

where $z_{\rm LS}$ denotes the redshift of last scattering. The function $E(z)$ denotes the Hubble parameter at redshift z normalized by its value today. In the NPDDE model it is given by

$$\begin{aligned} E(z) &= \frac{H(z)}{H_0} \\ &\simeq \sqrt{(\Omega_c+\Omega_b)(1+z)^3+\Omega_{\rm DE}(z)+\Omega_\nu(z)}. \end{aligned} \qquad (6)$$

In the above equation, Ω_c and Ω_b are the current cold dark matter and baryon energy densities, respectively, $\Omega_{\rm DE}(z)$ is the dark energy density given by Eq. (3), and $\Omega_\nu(z)$ is the neutrino energy density. At late times, after neutrinos become nonrelativistic, $\Omega_\nu h^2 \approx M_\nu(1+z)^3/93.14$ eV, where $h = H_0/(100\ {\rm km\,s^{-1}\,Mpc^{-1}})$. In writing Eq. (6), we are neglecting the contribution of the photon energy density Ω_γ, which is negligible at the redshifts under consideration.

It is easy to show that *the normalized expansion rate $E(z)$ at late times is higher in a NPDDE universe than in a ΛCDM one* for fixed values of Ω_c, Ω_b, M_ν, and $\Omega_{\rm DE,0}$, as we shall comment more on below and in Fig. 3. The integral in Eq. (5) at fixed M_ν is therefore smaller in the NPDDE case than in the ΛCDM one. In order to keep D_A fixed, one is left with the option of decreasing both H_0 and M_ν. This option is preferred over the choice where one parameter is decreased by a greater amount while the other parameter is kept fixed, since in the latter case the more sizable decrease of the first parameter can lead to undesired changes in other regions of the CMB spectra, despite Θ_s being kept fixed. One could argue that the same effect can be obtained by decreasing Ω_c and/or Ω_b. However, this choice would alter the redshift of matter-radiation equality, which is accurately constrained by the amplitude of the first acoustic peak in the CMB power spectrum. Therefore, it is not the preferred choice. This physical explanation for the shifts in the bounds of M_ν is fully supported by the results of our Monte Carlo analyses. In particular, we have verified that the posterior of Θ_s is nearly unchanged when moving from the ΛCDM scenario to the NPDDE model.

From the explanation above it follows that in NPDDE models we expect a lower Hubble constant H_0 and/or a lower sum of the neutrino masses M_ν compared to the ΛCDM case. The shifts in H_0 and M_ν are necessary to keep Θ_s fixed. Therefore, the very strong anticorrelation (degeneracy) between M_ν and H_0 present in ΛCDM is weakened in NPDDE models. Note also that in NPDDE models we expect a lower value of σ_8, thus reducing the tension between primary CMB and cluster counts/weak lensing measurements (see, e.g., [160–174] for some works examining this tension and possible solutions).

In Fig. 2 we show the two-dimensional joint H_0-M_ν posterior for the base data set. The blue contours are obtained in the ΛCDM model, the red contours in the NPDDE model where $w(z) \geq -1$, and the grey contours for the more generic w_0w_aCDM model where also $w(z) < -1$ is allowed. The horizontal dashed line corresponds to $M_{\nu,\rm min} \simeq 0.1$ eV, the minimal value allowed by neutrino oscillation data in the inverted ordering scenario. The difference between the blue contours (ΛCDM) and the red contours (NPDDE model) is compatible with the shifts in H_0 and M_ν required to keep Θ_s fixed. The green band in Fig. 2 corresponds to the 68% C.I. for H_0 inferred by direct measurements from the Hubble Space Telescope [175,176]. From Fig. 2, it is clear that the tension between direct measurements and cosmological estimates of H_0 is not resolved, and actually worsened, within a NPDDE model. The tension can be partially alleviated by a generic dark energy component (the w_0w_aCDM model) able to access the region $w(z) < -1$ (grey contours) [177–206].[7] We have checked that similar considerations apply to the corresponding contour plot obtained with the pol data set.

From Fig. 2 we also see that the anticorrelation (degeneracy) between M_ν and H_0 is weakened when moving from ΛCDM (blue contours) to NPDDE models (red contours).

[7] A notable exception to this statement is, however, provided by running vacuum models (RVM), motivated by quantum field theoretical considerations [207]. Studies have shown that RVMs, which appear to be statistically preferred over ΛCDM, can address the H_0 tension, but do so invoking a nonphantom dark energy component (with the value $w = -1$ being preferred; see, e.g., [173,174,208–215] for some recent works). Notice that RVMs point toward values of H_0 which are closer to the CMB inferred value.

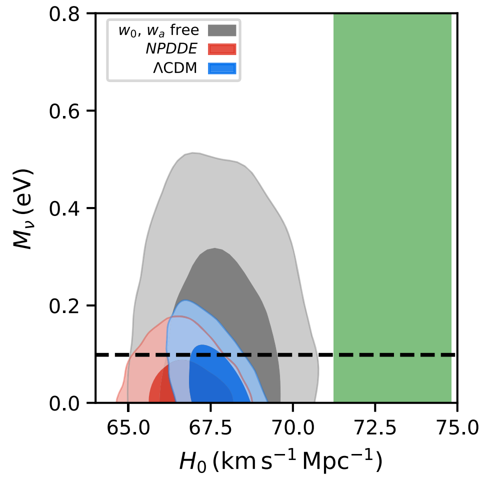

FIG. 2. Two-dimensional probability contours in the H_0-M_ν plane. The blue contours are obtained for the ΛCDM model, the red contours are for a dynamical dark energy model with EoS parametrized by Eq. (1) and satisfying $w(z) \geq -1$ (NPDDE), and the grey contours are for a generic dark energy model with EoS parametrized by Eq. (1). The green band indicates the 68% C.I. for H_0 from direct measurements of the Hubble Space Telescope [175,176]. The horizontal dashed line corresponds to $M_{\nu,\mathrm{min}} \simeq 0.1$ eV, the minimal value for the sum of the neutrino masses allowed in the inverted ordering scenario by neutrino oscillation data. When moving from the ΛCDM contours (blue) to models with $w(z) \geq -1$ (red), the shifts of H_0 and M_ν to smaller values are evident. These shifts are necessary to keep the angular scale of the sound horizon at recombination Θ_s fixed; see discussion in the main text. It is also clear that the M_ν-H_0 degeneracy is weakened when moving from ΛCDM to models with $w(z) \geq -1$ (NPDDE). For further information, see the discussion in the main text concerning the M_ν-H_0 correlation coefficient, which is reduced from −0.43 (ΛCDM) to −0.14 (NPDDE). The tension between direct measurements of H_0 and cosmological estimates is not resolved by a dark energy component with $w(z) \geq -1$. The tension is partially alleviated by a generic dark energy component which can access the $w(z) < -1$ region (grey contours). The contour regions are obtained for the base data set combination of CMB, BAO, and SNeIa data, with no CMB small scale polarization data. Similar considerations apply to the contours derived from the combination which also includes small scale CMB polarization data.

The magnitude of the degeneracy is reflected by the tilt of the main axes of the ellipsoidal M_ν-H_0 contours. The contour in the ΛCDM case is visibly more inclined than the NPDDE one. The weakening of the M_ν-H_0 degeneracy can be rigorously quantified by computing the correlation coefficient between the two parameters. The correlation coefficient between two parameters i and j, R_{ij}, is defined as $R_{ij} = C_{ij}/\sqrt{C_{ii}C_{jj}}$, where C is the covariance matrix of the cosmological parameters (in our case $i = M_\nu$ and $j = H_0$), estimated from our MCMC runs. For the base [pol] data set, we find a correlation coefficient of −0.43 [−0.50] in the ΛCDM case, which is lowered to −0.14 [−0.16] in the NPDDE case. Therefore, the correlation between the two parameters is strongly reduced in moving from ΛCDM to NPDDE models.

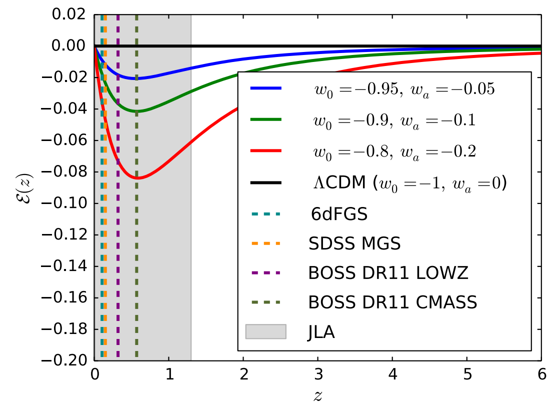

FIG. 3. $\mathcal{E}(z)$, defined in Eq. (7), quantifies the difference in the normalized expansion rate $H(z)/H_0$ between a dynamical dark energy model with equation of state $w(z) \geq -1$ (NPDDE) and a ΛCDM model. The quantity $\mathcal{E}(z)$ is plotted for sample cosmologies with $w_0 = -0.95, w_a = -0.05$ (blue curve), $w_0 = -0.9$, $w_a = -0.1$ (green curve), $w_0 = -0.8, w_a = -0.2$ (red curve), and $w_0 = -1, w_a = 0$ [black curve, ΛCDM, where $\mathcal{E}(z) = 0$]. We have fixed $\Omega_{m,0} = 0.3$ and $\Omega_{\mathrm{DE},0} = 0.7$. The negative $\mathcal{E}(z)$ indicates that the normalized expansion rate is higher in the NPDDE model compared to ΛCDM. The four vertical dashed lines indicate the redshift of the four BAO measurements we consider in this work: 6dFGS (cyan line), SDSS MGS (orange line), BOSS DR11 LOWZ (purple line), and BOSS DR11 CMASS (green line). The grey shaded band refers to the redshift coverage of the JLA Supernovae Ia sample. Thus the measurements considered in this work probe the redshift range in which the dip in $\mathcal{E}(z)$ is most prominent.

We shall now demonstrate that the late-time expansion rate $E(z)$ is higher in a Universe with $w(z) \geq -1$ compared to ΛCDM. We shall also identify the redshift range in which this effect is most prominent. We define the following quantity:

$$\mathcal{E}(z) \equiv \left(\frac{E(z)|_{\Lambda\mathrm{CDM}}}{E(z)|_{\mathrm{NPDDE}}}\right)^2\Bigg|_{\Omega_m,\Omega_{\mathrm{DE},0}} - 1, \tag{7}$$

where $|_{\Lambda\mathrm{CDM}}$ and $|_{\mathrm{NPDDE}}$ indicate that $E(z)$ is evaluated in a ΛCDM universe or in a universe with $w(z) \geq -1$, respectively. The notation $|_{\Omega_m,\Omega_{\mathrm{DE},0}}$ denotes that $\Omega_m = \Omega_c + \Omega_b + \Omega_\nu$ and $\Omega_{\mathrm{DE},0}$ are kept fixed when moving from ΛCDM to NPDDE. $\mathcal{E}(z) = 0$ therefore corresponds to the ΛCDM case. A negative $\mathcal{E}(z)$ instead indicates that the expansion rate normalized by H_0 is higher in the NPDDE model compared to ΛCDM. Note that $\mathcal{E}(z)$ is closely related to other diagnostics used in the literature to probe the DE evolution, such as the Om diagnostic [216]. In Fig. 3, $\mathcal{E}(z)$ is plotted for three choices of w_0, w_a. All of the choices satisfy the stability priors imposed by Eq. (2) and ensure that $w(z) \geq -1$.

Figure 3 clearly shows that $\mathcal{E}(z)$ is negative at low redshifts, as expected from the above discussion. $\mathcal{E}(z)$ also shows a minimum for $z \approx 0.5$ for values of w_0 and w_a that are allowed by cosmological data. The four vertical dashed lines indicate the redshift of the four BAO measurements we consider in this work. The grey shaded band refers to the redshift coverage of the JLA supernovae Type-Ia sample we consider in this analysis. Thus, we see that the measurements adopted in this work cover the redshift range where the difference between $\mathcal{E}(z)$ and $\mathcal{E}(z) = 0$ is largest. Therefore, the redshift range of current BAO and SNeIa measurements is ideal to probe the dynamics of nonphantom $[w(z) \geq -1]$ dark energy.

C. Comment on the Bayesian statistical approach adopted

Here we comment on the *a priori* counterintuitive fact that the bounds on M_ν in the NPDDE model are tighter than those in ΛCDM, despite the fact that ΛCDM represents the limiting case of NPDDE when $w_0 = -1$ and $w_a = 0$. Indeed, these tighter bounds are a result of our use of a Bayesian statistical approach [217,218].

To explain our results, we begin by *fixing* the parameters w_0 and w_a to specific values not corresponding to ΛCDM (i.e., $w_0 \neq -1$ and $w_a \neq 0$), yet still satisfying $w(z) \geq -1$. Following the explanation of the previous section, we expect that the bounds on M_ν must become ever tighter as the dark energy model gets farther away from ΛCDM. We will study specific cases below and find that these expectations are met. Therefore, a Bayesian analysis marginalizing over the range of w_0, w_a values satisfying $w(z) \geq -1$ is expected to obtain a bound on M_ν which is slightly tighter than the ΛCDM one, as shown by the results in Sec. IV A.

Specifically we considered four test cases: (a) $w_0 = -0.95$, $w_a = 0$, (b) $w_0 = -0.95$, $w_a = 0.05$, (c) $w_0 = -0.9$, $w_a = 0$, and (d) $w_0 = -0.85$, $w_a = 0$, and found 95% C.I. upper bounds of (a) $M_\nu < 0.13$ eV, (b) $M_\nu < 0.12$ eV, (c) $M_\nu < 0.11$ eV, and (d) $M_\nu < 0.08$ eV. Indeed, the bounds on neutrino mass are tighter than in the case of standard ΛCDM.

The posterior distributions of M_ν are shown in Fig. 4, in dashed light blue, dashed purple, dashed yellow, and dashed red lines for cases (a)–(d), respectively. The ΛCDM bound is instead represented by the solid black line. It is visually clear that the bounds for these cases are all tighter than the ΛCDM one. For pedagogical purposes we have also considered two cases where $w_0 \neq -1$ and $w_a \neq 0$ are instead fixed to values such that $w(z) \geq -1$ is not satisfied: (e) $w_0 = -1.05$, $w_a = 0$, and (f) $w_0 = -1.05$, $w_a = 0.05$. The corresponding posterior distributions are shown in dashed dark blue and dashed green lines in Fig. 4 and correspond to 95% C.I. upper bounds of (e) $M_\nu < 0.19$ eV and (f) $M_\nu < 0.18$ eV. As per our expectations, the bounds for cases (e) and (f) are looser than the ΛCDM one. To further back up this argument, we show a triangular plot in M_ν-w_0-w_a space in Fig. 5, where we compare constraints obtained assuming the w_0w_aCDM model (blue contours) and the NPDDE model (red contours). From there it is clear that restricting the allowed region to the NPDDE parameter space inevitably selects the region of parameter space with very low M_ν, due to the direction of the mutual M_ν-w_0-w_a degeneracies.

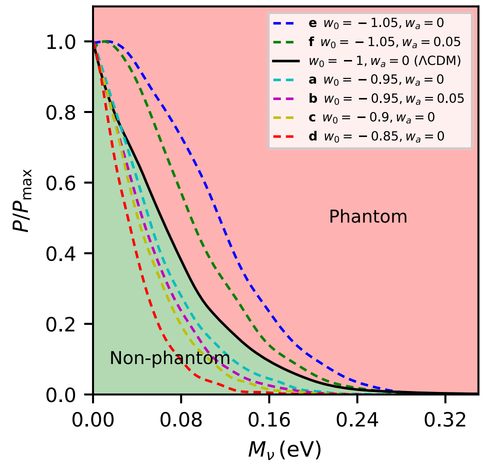

FIG. 4. One-dimensional posterior probabilities of the sum of the three active neutrino masses M_ν (in eV) for a selection of cosmological models with w_0 and w_a *fixed*, described in Sec. IV C. Models (a)–(d) have w_0 and w_a fixed to values satisfying the condition $w(z) \geq -1$, and are represented by the dashed light blue, dashed purple, dashed yellow, and dashed red curves, respectively. Models (e) and (f) have w_0 and w_a fixed to values not satisfying the condition $w(z) \geq -1$, and are represented by the dashed dark blue and dashed green curves, respectively. The ΛCDM result corresponds to the solid black line. The region where $w(z) \geq -1$ is satisfied is shaded in green and labeled “Non-phantom”; conversely, the region where $w(z) \geq -1$ is not satisfied is shaded in pink and labeled “Phantom.” It is clear that the bounds on M_ν for models where w_0 and w_a are fixed to values satisfying $w(z) \geq -1$ are always tighter than the ΛCDM bound. Therefore, a Bayesian analysis marginalizing over the range of w_0, w_a values satisfying $w(z) \geq -1$ is expected to obtain a bound on M_ν which is slightly tighter than the ΛCDM one, as shown by the results in Sec. IV A.

In the Bayesian statistical approach adopted to obtain the results in Sec. IV A, w_0 and w_a are not fixed, but rather varied. Subsequently, the uncertainty in w_0 and w_a is integrated out by the process of marginalization, leading to the marginalized posterior on M_ν. Heuristically, this procedure can be viewed as a weighted average over the range of prior possibilities of w_0 and w_a, with weights given by the value of the prior in that particular point of parameter space. For each of these prior possibilities of w_0 and w_a, we have already seen that the corresponding bound on M_ν is tighter than the ΛCDM bound; see examples (a)–(d) above as well as the green-shaded region in Fig. 4. Therefore, the weighted average of such bounds is expected to not be

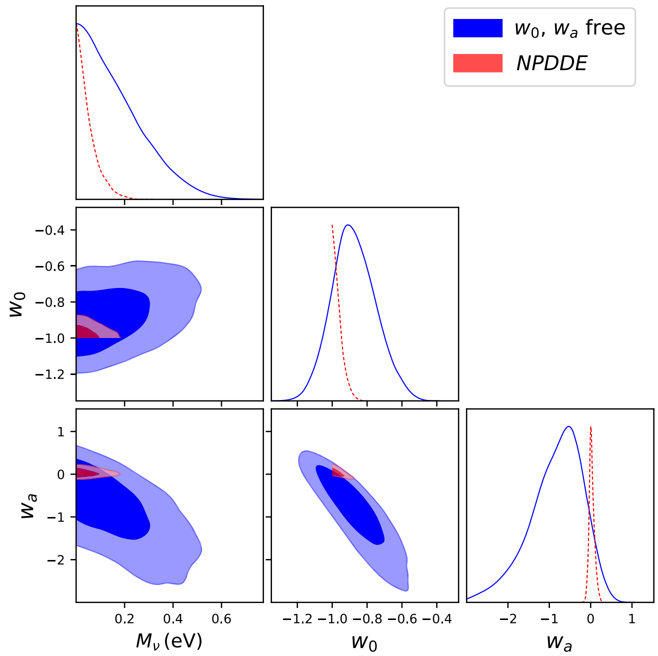

FIG. 5. The 68% C.I. (dark blue/red) and 95% C.I. (light blue/red) joint posterior distributions in the M_ν-w_0-w_a plane, along with their marginalized posterior distributions from the base data set, for the $w_0 w_a$CDM (blue contours) and NPDDE models (red contours). The marginalized posterior distributions appearing along the diagonal are normalizable probability distributions and hence in arbitrary units. The sharp cuts in the red posteriors are due to the hard NPDDE priors [see Eq. (2)].

weaker than the ΛCDM constraint, as confirmed by our results in Sec. IV A. This explains the *a priori* counterintuitive fact that the upper limits on M_ν for the NPDDE model are slightly tighter than the ΛCDM limit despite the enlarged parameter space.

D. Implications for the determination of the neutrino mass ordering

Finally, we comment on the implications that the results of this work could have for the determination of the neutrino mass ordering. By integrating the posterior distributions of M_ν for both the base and pol data sets (solid red and dashed red lines in Fig. 1, respectively) it is straightforward to show that a significant fraction ($\gtrsim 90\%$) of the M_ν posterior probability lies in the range $M_\nu < 0.1$ eV. This region is precluded to the inverted mass ordering by neutrino oscillation data.

Should noncosmological probes such as long-baseline neutrino oscillation experiments (e.g., T2K [219], NOvA [220], or DUNE [221]) establish that the neutrino mass ordering is inverted, the viability of dark energy models with $w(z) \geq -1$ could be jeopardized. This conclusion holds if we exclude exotic physics at play in the cosmological neutrino sector and/or in the gravitational sector. Examples of such exotic models are those with nonstandard neutrino interactions predicting a vanishing neutrino energy density today [158] or mass-varying neutrinos [222–225], and models of modified gravity where the bounds on M_ν could be significantly different from those in ΛCDM [226–234].

Therefore, we have brought to light a subtle and perhaps unexpected connection between two at first glance seemingly disconnected fields: neutrino oscillation experiments and the nature of dark energy. In the near future, results from the former might be able to shed important light on the latter. It is also worth noticing that our findings could also be very interesting in light of the recently revived Swampland conjectures [235–237] (see also, e.g., [238–250]), which suggest that it is not possible to construct metastable de Sitter vacua in a controlled way within string theory. As a corollary, if string theory is the correct high-energy description, the current period of accelerated expansion should be sourced by a quintessence field, e.g., through slowly rolling moduli fields which naturally arise in string compactification scenarios. If future long baseline experiments should find the neutrino mass ordering to be inverted, this scenario would naturally be put under pressure, with extremely interesting implications concerning viable high-energy theories.

Finally, we quantify the preference for the normal ordering within NPDDE models in terms of probability odds ($p_{\rm NO} : p_{\rm IO}$). We adopt the methodology outlined in Sec. III. For the NPDDE model, where $w(z) \geq -1$, we find that the normal ordering is mildly preferred with posterior odds ∼2∶1 for the base data set and ∼3∶1 for the pol data set.

We compare these figures to those obtained in the generic $w_0 w_a$CDM model. In this case, we find no preference for any of the two orderings for both the base and pol data sets (posterior odds of ∼1∶1). When assuming the standard ΛCDM cosmological scenario, we find a mild preference for normal ordering of ∼2∶1 for both the base and pol data set combinations.

Finally, in Appendix B, we provide an alternative approach to quantify the preference for the normal ordering. This alternative approach is based on the AIC estimator for the relative quality of statistical models. The findings are qualitatively in agreement with those reported in this section.

V. SUMMARY AND DISCUSSION

A DDE component driving cosmic acceleration provides an alternative to the cosmological constant. In this work, we have explored cosmological constraints on the sum of the three active neutrino masses M_ν within DDE models. We parametrize the dark energy EoS as a function of redshift z through the usual CPL parametrization $w(z) = w_0 + w_a z/(1+z)$. Furthermore, we impose the requirement that the EoS satisfies $w(z) \geq -1$ throughout the expansion history. We refer to this class of models as NPDDE. We employ a combination of CMB, BAO, and SNeIa measurements. We denote by base the data set combination not including CMB polarization data at small scales, and by pol the data set combination that includes these CMB polarization data.

The conclusions we reach are threefold:

(i) We find that the constraints on M_ν assuming a NPDDE model are slightly tighter than those obtained within the standard ΛCDM scenario. This is the opposite of what is found when a generic DDE model with EoS is allowed to enter the region where $w(z) < -1$ ($w_0 w_a$CDM model) is assumed. More in detail, we find 95% C.I. upper bounds of $M_\nu < 0.13$ eV for the base data set and $M_\nu < 0.11$ eV for the pol data set in a NPDDE model. These figures can be compared to the 95% C.I. upper bounds of $M_\nu < 0.16$ eV for the base data set and $M_\nu < 0.13$ eV for the pol data set in a ΛCDM model. For the $w_0 w_a$CDM model, we find instead the 95% C.I. upper bounds of $M_\nu < 0.41$ eV for the base data set and $M_\nu < 0.37$ eV for the pol data set. We provide a thorough data-supported physical and statistical explanation of these results. The explanation is based on the effects of massive neutrinos and dark energy on the background cosmological evolution, as well as on the Bayesian statistical method adopted.

(ii) A DDE component with $w(z) \geq -1$ does not alleviate the tension between cosmological and direct measurements of H_0, contrary to what is found in dark energy models with arbitrary $w(z)$. We find that NPDDE models prefer lower values of H_0 than those inferred by direct measurements. We also show that the well known degeneracy between H_0 and M_ν is reduced within NPDDE models. We provide a thorough explanation of this finding.

(iii) We combine the results of the cosmological analysis with neutrino oscillation data, and quantify the statistical preference for one of the two neutrino mass orderings over the other. The constraints on M_ν in NPDDE models correspond to probability odds of $\sim 2{:}1$ in favor of normal ordering with respect to inverted ordering for the base data set combination and $\sim 3{:}1$ for the pol data set. These odds show a mild preference for normal ordering. If laboratory experiments determine that the neutrino mass ordering is inverted, and if the current cosmic acceleration is caused by a dynamical dark energy component, this component would likely be phantom $[w(z) < -1]$, or at least have to cross the phantom divide at some point during the expansion history. The conclusion holds as long as we exclude nonstandard scenarios either in the neutrino sector or in the gravity sector. Therefore, this result brings to light a perhaps unexpected connection between two at first glance seemingly disconnected fields: neutrino oscillation experiments and the nature of dark energy. In the near future, results from the former might be able to shed important light on the latter.

ACKNOWLEDGMENTS

The authors thank Per Andersen, Thejs Brinckmann, Eleonora Di Valentino, Enrique Fernández Martínez, Edvard Mörtsell, Eiichiro Komatsu, Massimiliano Lattanzi, Eric Linder, Matteo Martinelli, Savvas Nesseris, Lorenzo Sebastiani, Zachary Slepian, Alessandra Silvestri, Michael Turner, and Sergio Zerbini for enlightening discussions. This work is based on observations obtained with Planck (www.esa.int/Planck), an ESA science mission with instruments and contributions directly funded by ESA Member States, NASA, and Canada. We acknowledge use of the Planck Legacy Archive. We also acknowledge the use of computing facilities at NERSC. K. F. acknowledges support from DOE Grant No. DE-SC0007859 at the University of Michigan as well as support from the Leinweber Center for Theoretical Physics. K. F., M. G., and S. V. acknowledge support by the Vetenskapsrå det (Swedish Research Council) through Contract No. 638-2013-8993 and the Oskar Klein Centre for Cosmoparticle Physics. S. D. and A. G. acknowledge support by the Vetenskapsrå det, the Swedish Space Board, and the K & A Wallenberg foundation. O. M. is supported by PROMETEO II/2014/050, by the Spanish Grant No. FPA2014–57816-P of the MINECO, by the MINECO Grant No. SEV-2014-0398, and by the European Union’s Horizon 2020 research and innovation programme under the Marie Skł odowska-Curie Grant Agreements No. 690575 and No. 674896. O. M. thanks the Fermilab Theoretical Physics Department for its hospitality.

Note added.—After our paper appeared on the arXiv, the work [251] appeared which considers also neutrino mass bounds within quintessence models. Their work differs from ours in the parametrizations adopted for w(z). Moreover, after our paper appeared on the arXiv, two further works [90,91] confirmed our result that the bounds on Mν in nonphantom dynamical dark energy models are tighter than those obtained in ΛCDM. All codes, chains, and scripts used to produce the results and plots of this work will be made publicly available at github.com/sunnyvagnozzi/NPDDE after acceptance of the paper in a journal.

APPENDIX A: INCLUDING THE NEUTRINO OSCILLATIONS LIKELIHOOD

Throughout this work, we have imposed a top-hat prior on M_ν of $M_\nu \geq 0$ eV. That is, we allowed values of M_ν below the minimum value set by oscillation experiments of 0.06 eV. The rationale behind this choice, as we outlined in Sec. III, was threefold:

(i) To obtain a bound relying *exclusively* on cosmological data.

(ii) To remain open to the possibility of models with nonstandard neutrino interactions leading to a neutrino energy density which is either vanishing or lower than the expectation in ΛCDM (e.g., [158]): at the level of cosmological data these effects can be phenomenologically captured by considering values of M_ν below the lower bound set by oscillation experiments.

(iii) To provide an (in)consistency test for DE models where the upper bound on M_ν ends up lying significantly below the lower bound set by oscillation experiments. While this possibility has not been realized in our work due to insufficient sensitivity, it might be realized in the near future thanks to dramatic improvements in the sensitivity of future CMB, large-scale structure, and supernovae distance measurements data sets.

Moreover, as also explained in Sec. III, the positivity of M_ν is the only genuine *a priori* information present in the problem, whereas the information that $M_\nu \geq 0.06$ eV is not truly *a priori*, but rather *a posteriori* of oscillation experiments. Therefore, the formally correct way of incorporating such information is, in fact, by including the neutrino oscillations likelihood. In addition, as discussed in Sec. III, as far as upper limits on M_ν (which are the subject of this work) are concerned, the oscillations likelihood can be to zeroth approximation included as a sharp cutoff at $M_\nu = 0.06$ eV, because the uncertainty to which $M_{\nu,\mathrm{min}} \simeq 0.06$ eV is subject is extremely tiny (but an uncertainty is nonetheless present, whereas the physical lower bound $M_\nu \geq 0$ eV is instead subject to no uncertainty). Let us first discuss this simplified case where the oscillations likelihood is simply included as a sharp cutoff in the M_ν prior, before discussing a more physical, but still simple, way of including the oscillations likelihood.

One might at this point wonder whether our results are dependent on the choice of prior: $M_\nu \geq 0$ eV versus $M_\nu \geq 0.06$ eV. In fact, the specific bounds on M_ν within a given model (in this case, w_0w_aCDM, ΛCDM, and NPDDE) *are* certainly affected by the choice of prior. Nonetheless, it is easy to show that if the prior on M_ν is chosen to be flat even when the lower bound from oscillation experiments is enforced, then as a consequence of Bayes' theorem the key result of our paper remains unchanged. That is, the constraints on M_ν in NPDDE models remain tighter than those obtained in ΛCDM, even when the lower limit of $M_\nu \geq 0.06$ eV is enforced.

Let us denote by $\boldsymbol{x}$ our data and by $\boldsymbol{\theta}$ the set of cosmological parameters excluding M_ν. Let us further denote by $\mathcal{L}(\boldsymbol{x}|M_\nu,\boldsymbol{\theta})$ our likelihood, and by $\pi(M_\nu)$ and $\pi(\boldsymbol{\theta})$ the prior distributions on M_ν and $\boldsymbol{\theta}$, respectively. Note that we are implicitly assuming that the prior on M_ν can be factorized from the prior on the other cosmological parameters, an assumption that is realized. From Bayes' theorem we know that the posterior distribution of M_ν given the data, $p(M_\nu|\boldsymbol{x})$, is given by the following:

$$p(M_\nu|\boldsymbol{x}) \propto \int d\boldsymbol{\theta}\mathcal{L}(\boldsymbol{x}|M_\nu,\boldsymbol{\theta})\pi(M_\nu)\pi(\boldsymbol{\theta}). \qquad \text{(A1)}$$

Assuming we keep a flat prior on M_ν, the only effect of imposing the lower limit from oscillation experiments is to cut $\pi(M_\nu)$ at 0.06 eV instead of 0 eV. From Eq. (A1), we see that the result of this operation would be to shift the posterior of M_ν to higher values: this will affect all quantities computed from the distribution, such as the mean and the 95% C.I. upper bound, both of which would increase, hence leading to broader constraints.

However, in our work we are not interested in the bounds on M_ν *per se*. The purpose of our work is to examine how the upper limits on M_ν change when moving from ΛCDM to NPDDE. In Fig. 1, we showed how the posterior of M_ν obtained assuming the NPDDE model is shifted to lower values compared to the one obtained assuming the ΛCDM model. From Eq. (A1), it is easy to see how this fact continues to be true even when the lower limit of 0.06 eV set by oscillation experiments is imposed. Therefore, we expect as a consequence of Bayes' theorem that the upper limits on M_ν in NPDDE models will still be tighter than those obtained in ΛCDM regardless of whether a prior of $M_\nu \geq 0$ eV or $M_\nu \geq 0.06$ eV is chosen.

To confirm the above statement explicitly, we recompute the posteriors and upper limits on M_ν obtained in Sec. IV, this time imposing the lower limit set by oscillation experiments. We recomputed the bounds only for the ΛCDM and NPDDE models (leaving aside w_0w_aCDM, since it is not important for our conclusions), and only for the base data set (since the pol data set leads to identical conclusions). For the ΛCDM case, we find that the 95% C.I. upper bound of 0.16 eV degrades to 0.19 eV when imposing $M_\nu \geq 0.06$ eV. Similarly, when considering the NPDDE model, the limit degrades from 0.13 eV to 0.17 eV. However, we see that in both cases the upper limit obtained assuming NPDDE is tighter than that obtained assuming ΛCDM, confirming the conclusion we reached previously on the basis of Bayes' theorem.

Recall also that we computed the posterior odds for normal ordering versus inverted ordering using the methodology of [123] outlined in Sec. III. We wish to clarify that the posterior odds computed in this way are not affected by the choice of prior on M_ν. The reason is that, in Eq. (4), the likelihood of the cosmological data $\mathcal{L}(D|m_0,O)$ has been rewritten in terms of the mass of the lightest neutrino mass eigenstate m_0 rather than the total neutrino mass M_ν. The relation between M_ν involves the squared mass splittings measured by oscillation experiments. Therefore, the methodology adopted factors in, by construction, the information concerning the lower limits on M_ν set for the normal and inverted orderings. As a result, this methodology automatically ignores the region of the M_ν posterior which lies below 0.06 eV. In fact, it is easy to show that in the low-mass region of M_ν parameter space favored by data,

$M_\nu \lesssim 0.15$ eV, the posterior odds for normal versus inverted ordering calculated using Eq. (4) are well approximated by the following [66]:

$$\frac{p_N}{p_O} \approx \frac{\int_{0.06\ \mathrm{eV}}^{\infty} dM_\nu p(M_\nu|\boldsymbol{x})}{\int_{0.10\ \mathrm{eV}}^{\infty} dM_\nu p(M_\nu|\boldsymbol{x})}, \tag{A2}$$

where $p(M_\nu|\boldsymbol{x})$ is the posterior of M_ν. The form of Eq. (A2) shows how the information on the lower limits of M_ν for both the normal and the inverted ordering enters by construction in the methodology adopted.

So far, we considered the extremely simplified case where the information from oscillation experiments is included as a sharp cutoff in the M_ν prior. In fact, the minimum value allowed by oscillation experiments does not come without uncertainty. Using the best-fit values and 1σ intervals from [122] for the two mass-squared splittings assuming the normal ordering, we find $M_{\nu,\mathrm{min}} \approx 0.0589 \pm 0.0005$ eV. Therefore, we can to first approximation treat the oscillations likelihood as being a constant down to 0.0589 eV, and as a truncated Gaussian centered at 0.0589 eV and with width 0.0005 eV below. If we simply included the oscillations likelihood as a sharp cutoff, the result on the M_ν posterior would be a sharp drop at 0.06 eV, which is in a sense "unphysical" because this cutoff is actually induced by the value of $M_{\nu,\mathrm{min}}$ inferred from oscillation experiments with some uncertainty, and not by a physical lower bound that comes without uncertainty (such as $M_\nu \geq 0$ eV). Nonetheless, since $M_{\nu,\mathrm{min}}$ is known to better than $\approx$0.8% precision, it is perfectly reasonable to expect that the impact on the upper limits on M_ν of using our smeared Gaussian approximation versus a sharp cutoff is going to be negligible at best (which we later confirm).

In Fig. 6, we show the posteriors we obtained for the ΛCDM (blue curves) and NPDDE (red curves) models, for both the case where the oscillations likelihood is not included (dashed curve) and the case where it is included (solid curve). We immediately notice two things. The first is that, as expected, the posterior drops very sharply below 0.0589 eV, signaling that the sharp cutoff approximation to the oscillations likelihood is, in fact, a reasonable approximation, given the extremely tiny uncertainty on $M_{\nu,\mathrm{min}}$. In fact, we find that we recover the upper limits we computed previously from the sharp cutoff approximation (0.17 eV for the NPDDE model and 0.19 eV for the ΛCDM model). The second observation is that, independently of whether the oscillations likelihood is included, the NPDDE posterior is always shifted to lower values of M_ν compared to the ΛCDM one, showing that the main conclusions of our paper are stable against the inclusion of the oscillations likelihood.

To conclude, we summarize the findings of this Appendix. The key conclusion of our work, namely the fact that the upper limits on M_ν are tighter in NPDDE models compared to ΛCDM, persists even when the oscillations likelihood is included. Approximating the oscillations likelihood as a sharp cutoff in M_ν (which we have argued is a reasonable zeroth approximation given the very tiny uncertainty on $M_{\nu,\mathrm{min}}$), we have shown how this result follows simply from Bayes' theorem. Using a more realistic approximation to the oscillations likelihood (treated as a truncated Gaussian), we show the impact of including this likelihood on the M_ν posterior in Fig. 6. Since the methodology adopted to compute the posterior odds of normal versus inverted ordering (see Sec. III and [123]) by construction takes into account the lower limits on M_ν coming from oscillation experiments for both normal and inverted ordering, the results obtained in Sec. IV D are unaffected by whether the lower limit of $M_\nu \geq 0.06$ eV is enforced. Therefore, in NPDDE models (and using the base data set), the preference for normal versus inverted ordering is ∼2:1.

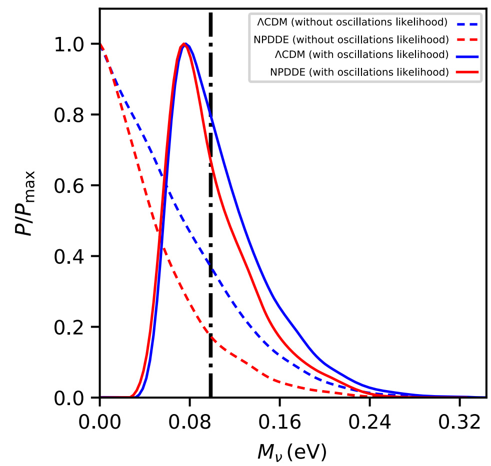

FIG. 6. One-dimensional posterior probabilities of the sum of the three active neutrino masses M_ν (in eV) for two models: the ΛCDM case (in blue curves), and the NPDDE model with $w(z) \geq -1$ (in red curves), considering both the case when the oscillations likelihood is not included (dashed curves) and the case where it is included (solid curves). We approximate the oscillations likelihood as being a constant for $M_\nu \geq 0.0589$ eV and a truncated Gaussian with width 0.0005 eV for $M_\nu < 0.0589$ eV. The vertical black dot-dashed line corresponds to the minimal mass of $M_{\nu,\mathrm{min}} \approx 0.1$ eV allowed by neutrino oscillation data within the inverted ordering. We visually see that the dashed/solid red curves are always shifted to lower values of M_ν compared to the respective dashed/solid blue curves. Therefore, the upper limits on M_ν are always tighter in the NPDDE model compared to the ΛCDM one, independently of whether the oscillations likelihood is included.

APPENDIX B: ESTIMATING THE PREFERENCE FOR THE NORMAL ORDERING THROUGH THE AKAIKE INFORMATION CRITERION

We complete the analysis of this work by quantifying the preference for one neutrino mass ordering over the other using an alternative statistical method based on the

AIC [252]. The AIC is a statistical indicator that estimates the relative statistical quality of different models. We use the AIC to estimate the preference for the NO against the IO. For a model with k parameters and log-likelihood $\ln(\mathcal{L}) = -\chi^2/2$, the AIC is given by

$$\mathrm{AIC} = 2k + \min(\chi^2), \tag{B1}$$

where $\min(\chi^2)$ denotes the minimum value of the χ^2 for the model. The difference between the AICs of two models, ΔAIC, estimates the relative quality of one model against the other. In particular, the model with the lowest AIC is to be considered statistically preferred.

As in Sec. IV, we combine results from cosmology and neutrino oscillation experiments to quantify the preference for the normal ordering. We obtain the posterior probability distribution of M_ν from the cosmological analysis and interpret this posterior as a likelihood for the cosmological data set (as done in [66,123]). From oscillation measurements, we take the one-dimensional χ^2 projections for the solar and atmospheric mass splittings computed separately for NO and IO, as provided by NuFIT 3.0 (2016) [120]. We then compute the global $\min(\chi^2)$ for both NO and IO in light of the combination of cosmological and oscillation data.

The number of parameters k is the same in the two scenarios; therefore, $\Delta\mathrm{AIC} = \Delta\min(\chi^2)$. For NPDDE models, we find $\Delta\mathrm{AIC} = \mathrm{AIC}_{\mathrm{IO}} - \mathrm{AIC}_{\mathrm{NO}} = 3.4$ for the base data set and $\Delta\mathrm{AIC} = 3.7$ for the pol data set. These values show a mild preference for the NO model, using the scale provided by [253]. In ΛCDM, we find $\Delta\mathrm{AIC} = 2.7$ for the base data set and $\Delta\mathrm{AIC} = 3.1$ for the pol data set. In this case, the preference for NO is even milder. Finally, in generic DDE models with arbitrary EoS, we find $\Delta\mathrm{AIC} = 1.9$ for the base data set and $\Delta\mathrm{AIC} = 2.0$ for the pol data set. We interpret these values as a minimal preference for NO. The results obtained using the AIC method are qualitatively in agreement with those obtained performing a Bayesian model comparison and reported in Sec. IV. Both indicate that current cosmological data, when interpreted in light of a NPDDE model, show a mild preference for the NO.

[1] A. G. Riess *et al.* (Supernova Search Team Collaboration), Observational evidence from supernovae for an accelerating universe and a cosmological constant, Astron. J. **116**, 1009 (1998).

[2] S. Perlmutter *et al.* (Supernova Cosmology Project Collaboration), Measurements of Omega and Lambda from 42 high redshift supernovae, Astrophys. J. **517**, 565 (1999).

[3] P. Astier and R. Pain, Observational evidence of the accelerated expansion of the Universe, C.R. Phys. **13**, 521 (2012).

[4] P. A. R. Ade *et al.* (Planck Collaboration), Planck 2015 results. XIII. Cosmological parameters, Astron. Astrophys. **594**, A13 (2016).

[5] S. Alam *et al.* (BOSS Collaboration), The clustering of galaxies in the completed SDSS-III Baryon Oscillation Spectroscopic Survey: Cosmological analysis of the DR12 galaxy sample, Mon. Not. R. Astron. Soc. **470**, 2617 (2017).

[6] T. M. C. Abbott *et al.* (DES Collaboration), Dark Energy Survey year 1 results: Cosmological constraints from galaxy clustering and weak lensing, Phys. Rev. D **98**, 043526 (2018).

[7] V. Sahni, Dark matter and dark energy, Lect. Notes Phys. **653**, 141 (2004).

[8] S. Nojiri and S. D. Odintsov, Introduction to modified gravity and gravitational alternative for dark energy, eConf **C0602061**, 06 (2006) [Int. J. Geom. Methods Mod. Phys. **04**, 115 (2007)].

[9] J. Frieman, M. Turner, and D. Huterer, Dark energy and the accelerating universe, Annu. Rev. Astron. Astrophys. **46**, 385 (2008).

[10] K. Bamba, S. Capozziello, S. Nojiri, and S. D. Odintsov, Dark energy cosmology: The equivalent description via different theoretical models and cosmography tests, Astrophys. Space Sci. **342**, 155 (2012).

[11] M. J. Mortonson, D. H. Weinberg, and M. White, Dark energy: A short review, arXiv:1401.0046.

[12] D. Huterer and D. L. Shafer, Dark energy two decades after: Observables, probes, consistency tests, Rep. Prog. Phys. **81**, 016901 (2018).

[13] J. T. Nielsen, A. Guffanti, and S. Sarkar, Marginal evidence for cosmic acceleration from Type Ia supernovae, Sci. Rep. **6**, 35596 (2016).

[14] B. S. Haridasu, V. V. Luković, R. D'Agostino, and N. Vittorio, Strong evidence for an accelerating universe, Astron. Astrophys. **600**, L1 (2017).

[15] S. Dhawan, A. Goobar, E. Mörtsell, R. Amanullah, and U. Feindt, Narrowing down the possible explanations of cosmic acceleration with geometric probes, J. Cosmol. Astropart. Phys. 07 (2017) 040.

[16] I. Tutusaus, B. Lamine, A. Dupays, and A. Blanchard, Is cosmic acceleration proven by local cosmological probes?, Astron. Astrophys. **602**, A73 (2017).

[17] L. H. Dam, A. Heinesen, and D. L. Wiltshire, Apparent cosmic acceleration from type Ia supernovae, Mon. Not. R. Astron. Soc. **472**, 835 (2017).

[18] P. Andersen and J. Hjorth, Discerning dark energy models with high-redshift standard candles, Mon. Not. R. Astron. Soc. **472**, 1413 (2017).

[19] I. Tutusaus, B. Lamine, and A. Blanchard, Model-independent cosmic acceleration and type Ia supernovae

intrinsic luminosity redshift dependence, arXiv:1803.06197.
[20] S. Weinberg, The cosmological constant problem, Rev. Mod. Phys. **61**, 1 (1989).
[21] S. M. Carroll, The cosmological constant, Living Rev. Relativity **4**, 1 (2001).
[22] P. J. E. Peebles and B. Ratra, The cosmological constant and dark energy, Rev. Mod. Phys. **75**, 559 (2003).
[23] J. Martin, Everything you always wanted to know about the cosmological constant problem (but were afraid to ask), C.R. Phys. **13**, 566 (2012).
[24] P. J. E. Peebles and B. Ratra, Cosmology with a time variable cosmological constant, Astrophys. J. **325**, L17 (1988).
[25] V. Sahni and A. Starobinsky, The case for a positive cosmological Lambda term, Int. J. Mod. Phys. D **9**, 373 (2000).
[26] E. J. Copeland, M. Sami, and S. Tsujikawa, Dynamics of dark energy, Int. J. Mod. Phys. D **15**, 1753 (2006).
[27] R. R. Caldwell, A phantom menace?, Phys. Lett. B **545**, 23 (2002).
[28] E. Elizalde, S. Nojiri, and S. D. Odintsov, Late-time cosmology in (phantom) scalar-tensor theory: Dark energy and the cosmic speed-up, Phys. Rev. D **70**, 043539 (2004).
[29] A. Vikman, Can dark energy evolve to the phantom?, Phys. Rev. D **71**, 023515 (2005).
[30] S. Nojiri, S. D. Odintsov, and S. Tsujikawa, Properties of singularities in (phantom) dark energy universe, Phys. Rev. D **71**, 063004 (2005).
[31] F. Briscese, E. Elizalde, S. Nojiri, and S. D. Odintsov, Phantom scalar dark energy as modified gravity: Understanding the origin of the big rip singularity, Phys. Lett. B **646**, 105 (2007).
[32] S. Jhingan, S. Nojiri, S. D. Odintsov, M. Sami, I. Thongkool, and S. Zerbini, Phantom and non-phantom dark energy: The cosmological relevance of non-locally corrected gravity, Phys. Lett. B **663**, 424 (2008).
[33] S. Nojiri and E. N. Saridakis, Phantom without ghost, Astrophys. Space Sci. **347**, 221 (2013).
[34] D. L. Shafer and D. Huterer, Chasing the phantom: A closer look at Type Ia supernovae and the dark energy equation of state, Phys. Rev. D **89**, 063510 (2014).
[35] K. J. Ludwick, Examining the viability of phantom dark energy, Phys. Rev. D **92**, 063019 (2015).
[36] K. J. Ludwick, The viability of phantom dark energy: A review, Mod. Phys. Lett. A **32**, 1730025 (2017).
[37] G. Barenboim, W. H. Kinney, and M. J. P. Morse, Phantom Dirac-Born-Infeld dark energy, arXiv:1710.04458.
[38] S. W. Hawking and G. F. R. Ellis, *The Large Scale Structure of Space-Time*, Cambridge Monographs on Mathematical Physics (Cambridge University Press, Cambridge, UK, 2011).
[39] R. R. Caldwell, M. Kamionkowski, and N. N. Weinberg, Phantom Energy and Cosmic Doomsday, Phys. Rev. Lett. **91**, 071301 (2003).
[40] P. H. Frampton, K. J. Ludwick, and R. J. Scherrer, The little rip, Phys. Rev. D **84**, 063003 (2011).
[41] M. von Strauss, A. Schmidt-May, J. Enander, E. Mortsell, and S. F. Hassan, Cosmological solutions in bimetric gravity and their observational tests, J. Cosmol. Astropart. Phys. 03 (2012) 042.
[42] Y. Akrami, S. F. Hassan, F. Könnig, A. Schmidt-May, and A. R. Solomon, Bimetric gravity is cosmologically viable, Phys. Lett. B **748**, 37 (2015).
[43] A. Schmidt-May and M. von Strauss, Recent developments in bimetric theory, J. Phys. A **49**, 183001 (2016).
[44] E. Mortsell, Cosmological histories in bimetric gravity: A graphical approach, J. Cosmol. Astropart. Phys. 02 (2017) 051.
[45] A. V. Astashenok, S. Nojiri, S. D. Odintsov, and A. V. Yurov, Phantom cosmology without big rip singularity, Phys. Lett. B **709**, 396 (2012).
[46] R. Myrzakulov, L. Sebastiani, and S. Zerbini, Inhomogeneous viscous fluids in FRW universe, Galaxies **1**, 83 (2013).
[47] S. D. Odintsov and V. K. Oikonomou, Bouncing cosmology with future singularity from modified gravity, Phys. Rev. D **92**, 024016 (2015).
[48] V. K. Oikonomou, Singular bouncing cosmology from Gauss-Bonnet modified gravity, Phys. Rev. D **92**, 124027 (2015).
[49] S. D. Odintsov and V. K. Oikonomou, Big-bounce with finite-time singularity: The $F(R)$ gravity description, Int. J. Mod. Phys. D **26**, 1750085 (2017).
[50] M. Bouhmadi-Lopez and J. A. Jimenez Madrid, Escaping the big rip?, J. Cosmol. Astropart. Phys. 05 (2005) 005.
[51] C. Cattoen and M. Visser, Necessary and sufficient conditions for big bangs, bounces, crunches, rips, sudden singularities, and extremality events, Classical Quantum Gravity **22**, 4913 (2005).
[52] H. Wei and R.-G. Cai, Cosmological evolution of hessence dark energy and avoidance of big rip, Phys. Rev. D **72**, 123507 (2005).
[53] M. Bouhmadi-Lopez, P. F. Gonzalez-Diaz, and P. Martin-Moruno, Worse than a big rip?, Phys. Lett. B **659**, 1 (2008).
[54] X. Zhang, Heal the world: Avoiding the cosmic doomsday in the holographic dark energy model, Phys. Lett. B **683**, 81 (2010).
[55] B. Ratra and P. J. E. Peebles, Cosmological consequences of a rolling homogeneous scalar field, Phys. Rev. D **37**, 3406 (1988).
[56] R. R. Caldwell, R. Dave, and P. J. Steinhardt, Cosmological Imprint of an Energy Component with General Equation of State, Phys. Rev. Lett. **80**, 1582 (1998).
[57] R. R. Caldwell and E. V. Linder, The Limits of Quintessence, Phys. Rev. Lett. **95**, 141301 (2005).
[58] E. V. Linder, The dynamics of quintessence, the quintessence of dynamics, Gen. Relativ. Gravit. **40**, 329 (2008).
[59] K. Freese and M. Lewis, Cardassian expansion: A model in which the universe is flat, matter dominated, and accelerating, Phys. Lett. B **540**, 1 (2002).
[60] P. Gondolo and K. Freese, Fluid interpretation of Cardassian expansion, Phys. Rev. D **68**, 063509 (2003).
[61] K. Freese, Cardassian expansion: Dark energy density from modified Friedmann equations, New Astron. Rev. **49**, 103 (2005).

[62] N. Palanque-Delabrouille *et al.*, Neutrino masses and cosmology with Lyman-alpha forest power spectrum, J. Cosmol. Astropart. Phys. 11 (**2015**) 011.
[63] A. J. Cuesta, V. Niro, and L. Verde, Neutrino mass limits: Robust information from the power spectrum of galaxy surveys, Phys. Dark Universe **13**, 77 (2016).
[64] Q.-G. Huang, K. Wang, and S. Wang, Constraints on the neutrino mass and mass hierarchy from cosmological observations, Eur. Phys. J. C **76**, 489 (2016).
[65] E. Giusarma, M. Gerbino, O. Mena, S. Vagnozzi, S. Ho, and K. Freese, Improvement of cosmological neutrino mass bounds, Phys. Rev. D **94**, 083522 (2016).
[66] S. Vagnozzi, E. Giusarma, O. Mena, K. Freese, M. Gerbino, S. Ho, and M. Lattanzi, Unveiling ν secrets with cosmological data: Neutrino masses and mass hierarchy, Phys. Rev. D **96**, 123503 (2017).
[67] Z. Pan and L. Knox, Constraints on neutrino mass from cosmic microwave background and large scale structure, Mon. Not. R. Astron. Soc. **454**, 3200 (2015).
[68] M. Gerbino, M. Lattanzi, and A. Melchiorri, ν generation: Present and future constraints on neutrino masses from global analysis of cosmology and laboratory experiments, Phys. Rev. D **93**, 033001 (2016).
[69] E. Di Valentino, E. Giusarma, M. Lattanzi, O. Mena, A. Melchiorri, and J. Silk, Cosmological axion and neutrino mass constraints from Planck 2015 temperature and polarization data, Phys. Lett. B **752**, 182 (2016).
[70] R. Allison, P. Caucal, E. Calabrese, J. Dunkley, and T. Louis, Towards a cosmological neutrino mass detection, Phys. Rev. D **92**, 123535 (2015).
[71] M. Moresco, R. Jimenez, L. Verde, A. Cimatti, L. Pozzetti, C. Maraston, and D. Thomas, Constraining the time evolution of dark energy, curvature and neutrino properties with cosmic chronometers, J. Cosmol. Astropart. Phys. 12 (2016) 039.
[72] M. Oh and Y.-S. Song, Measuring neutrino mass imprinted on the anisotropic galaxy clustering, J. Cosmol. Astropart. Phys. 04 (2017) 020.
[73] M. Archidiacono, T. Brinckmann, J. Lesgourgues, and V. Poulin, Physical effects involved in the measurements of neutrino masses with future cosmological data, J. Cosmol. Astropart. Phys. 02 (2017) 052.
[74] F. Capozzi, E. Di Valentino, E. Lisi, A. Marrone, A. Melchiorri, and A. Palazzo, Global constraints on absolute neutrino masses and their ordering, Phys. Rev. D **95**, 096014 (2017).
[75] F. Couchot, S. Henrot-Versillé, O. Perdereau, S. Plaszczynski, B. Rouillé d'Orfeuil, M. Spinelli, and M. Tristram, Cosmological constraints on the neutrino mass including systematic uncertainties, Astron. Astrophys. **606**, A104 (2017).
[76] A. Caldwell, A. Merle, O. Schulz, and M. Totzauer, Global Bayesian analysis of neutrino mass data, Phys. Rev. D **96**, 073001 (2017).
[77] C. Doux, M. Penna-Lima, S. D. P. Vitenti, J. Tréguer, E. Aubourg, and K. Ganga, Cosmological constraints from a joint analysis of cosmic microwave background and large-scale structure, arXiv:1706.04583.
[78] S. Wang, Y.-F. Wang, and D.-M. Xia, Constraints on the sum of neutrino masses using cosmological data including the latest extended Baryon Oscillation Spectroscopic Survey DR14 quasar sample, Chin. Phys. C **42**, 065103 (2018).
[79] L. Chen, Q.-G. Huang, and K. Wang, New cosmological constraints with extended-Baryon Oscillation Spectroscopic Survey DR14 quasar sample, Eur. Phys. J. C **77**, 762 (2017).
[80] A. Upadhye, Neutrino mass and dark energy constraints from redshift-space distortions, arXiv:1707.09354.
[81] L. Salvati, M. Douspis, and N. Aghanim, Constraints from thermal Sunyaev-Zeldovich cluster counts and power spectrum combined with CMB, Astron. Astrophys. **614**, A13 (2018).
[82] R. C. Nunes and A. Bonilla, Probing the properties of relic neutrinos using the cosmic microwave background, the Hubble Space Telescope and galaxy clusters, Mon. Not. R. Astron. Soc. **473**, 4404 (2018).
[83] R. Emami *et al.*, Evidence of neutrino enhanced clustering in a complete sample of Sloan Survey Clusters, implying $\sum m_\nu = 0.11 \pm 0.03 eV$, arXiv:1711.05210.
[84] A. Boyle and E. Komatsu, Deconstructing the neutrino mass constraint from galaxy redshift surveys, J. Cosmol. Astropart. Phys. 03 (2018) 035.
[85] M. Zennaro, J. Bel, J. Dossett, C. Carbone, and L. Guzzo, Cosmological constraints from galaxy clustering in the presence of massive neutrinos, Mon. Not. R. Astron. Soc. **477**, 491 (2018).
[86] T. Sprenger, M. Archidiacono, T. Brinckmann, S. Clesse, and J. Lesgourgues, Cosmology in the era of Euclid and the Square Kilometre Array, arXiv:1801.08331.
[87] L.-F. Wang, X.-N. Zhang, J.-F. Zhang, and X. Zhang, Impacts of gravitational-wave standard siren observation of the Einstein Telescope on weighing neutrinos in cosmology, Phys. Lett. B **782**, 87 (2018).
[88] E. Giusarma *et al.*, Scale-dependent galaxy bias, CMB lensing-galaxy cross-correlation, and neutrino masses, arXiv:1802.08694.
[89] S. Mishra-Sharma, D. Alonso, and J. Dunkley, Neutrino masses and beyond: ΛCDM cosmology with LSST and future CMB experiments, Phys. Rev. D **97**, 123544 (2018).
[90] S. Roy Choudhury and S. Choubey, Updated bounds on sum of neutrino masses in various cosmological scenarios, J. Cosmol. Astropart. Phys. 09 (2018) 017.
[91] S. R. Choudhury and A. Naskar, Bounds on sum of neutrino masses in a 12 parameter extended scenario with non-phantom dynamical dark energy ($w(z) \geq -1$), arXiv:1807.02860.
[92] S. Vagnozzi, T. Brinckmann, M. Archidiacono, K. Freese, M. Gerbino, J. Lesgourgues, and T. Sprenger, Bias due to neutrinos must not uncorrect'd go, J. Cosmol. Astropart. Phys. 09 (2018) 001.
[93] N. Aghanim *et al.* (Planck Collaboration), Planck 2018 results. VI. Cosmological parameters, arXiv:1807.06209.
[94] T. Brinckmann, D. C. Hooper, M. Archidiacono, J. Lesgourgues, and T. Sprenger, The promising future of a robust cosmological neutrino mass measurement, arXiv:1808.05955.
[95] J. Aguirre *et al.* (Simons Observatory Collaboration), The Simons Observatory: Science goals and forecasts, arXiv:1808.07445.

[96] C. D. Kreisch *et al.*, Massive neutrinos leave fingerprints on cosmic voids, arXiv:1808.07464.

[97] M. Chevallier and D. Polarski, Accelerating universes with scaling dark matter, Int. J. Mod. Phys. D **10**, 213 (2001).

[98] E. V. Linder, Exploring the Expansion History of the Universe, Phys. Rev. Lett. **90**, 091301 (2003).

[99] M. Archidiacono, E. Giusarma, A. Melchiorri, and O. Mena, Neutrino and dark radiation properties in light of recent CMB observations, Phys. Rev. D **87**, 103519 (2013).

[100] E. Giusarma, R. de Putter, S. Ho, and O. Mena, Constraints on neutrino masses from Planck and Galaxy Clustering data, Phys. Rev. D **88**, 063515 (2013).

[101] S. Hannestad, Neutrinos in cosmology, New J. Phys. **6**, 108 (2004).

[102] J. Lesgourgues and S. Pastor, Massive neutrinos and cosmology, Phys. Rep. **429**, 307 (2006).

[103] S. Hannestad, Neutrino physics from precision cosmology, Prog. Part. Nucl. Phys. **65**, 185 (2010).

[104] Y. Y. Y. Wong, Neutrino mass in cosmology: Status and prospects, Annu. Rev. Nucl. Part. Sci. **61**, 69 (2011).

[105] J. Lesgourgues and S. Pastor, Neutrino mass from cosmology, Adv. High Energy Phys. **2012**, 608515 (2012).

[106] M. Archidiacono, T. Brinckmann, J. Lesgourgues, and V. Poulin, Neutrino properties from cosmology, arXiv:1705.00496.

[107] M. Lattanzi and M. Gerbino, Status of neutrino properties and future prospects—Cosmological and astrophysical constraints, Front. Phys. **5**, 70 (2018).

[108] S. Hannestad, Neutrino Masses and the Dark Energy Equation of State: Relaxing the Cosmological Neutrino Mass Bound, Phys. Rev. Lett. **95**, 221301 (2005).

[109] A. Goobar, S. Hannestad, E. Mortsell, and H. Tu, A new bound on the neutrino mass from the sdss baryon acoustic peak, J. Cosmol. Astropart. Phys. 06 (2006) 019.

[110] S. Joudaki, Constraints on neutrino mass and light degrees of freedom in extended cosmological parameter spaces, Phys. Rev. D **87**, 083523 (2013).

[111] C. S. Lorenz, E. Calabrese, and D. Alonso, Distinguishing between neutrinos and time-varying dark energy through cosmic time, Phys. Rev. D **96**, 043510 (2017).

[112] C. S. Lorenz, D. Alonso, and P. G. Ferreira, Impact of relativistic effects on cosmological parameter estimation, Phys. Rev. D **97**, 023537 (2018).

[113] W. Sutherland, The CMB neutrino mass/vacuum energy degeneracy: A simple derivation of the degeneracy slopes, Mon. Not. R. Astron. Soc. **477**, 1913 (2018).

[114] M. Sahlén, Cluster-void degeneracy breaking: Neutrino properties and dark energy, arXiv:1807.02470.

[115] M. C. Gonzalez-Garcia, M. Maltoni, J. Salvado, and T. Schwetz, Global fit to three neutrino mixing: Critical look at present precision, J. High Energy Phys. 12 (2012) 123.

[116] M. C. Gonzalez-Garcia, M. Maltoni, and T. Schwetz, Updated fit to three neutrino mixing: Status of leptonic *CP* violation, J. High Energy Phys. 11 (2014) 052.

[117] J. Bergstrom, M. C. Gonzalez-Garcia, M. Maltoni, and T. Schwetz, Bayesian global analysis of neutrino oscillation data, J. High Energy Phys. 09 (2015) 200.

[118] M. C. Gonzalez-Garcia, M. Maltoni, and T. Schwetz, Global analyses of neutrino oscillation experiments, Nucl. Phys. **B908**, 199 (2016).

[119] F. Capozzi, E. Lisi, A. Marrone, D. Montanino, and A. Palazzo, Neutrino masses and mixings: Status of known and unknown 3ν parameters, Nucl. Phys. **B908**, 218 (2016).

[120] I. Esteban, M. C. Gonzalez-Garcia, M. Maltoni, I. Martinez-Soler, and T. Schwetz, Updated fit to three neutrino mixing: Exploring the accelerator-reactor complementarity, J. High Energy Phys. 01 (2017) 087.

[121] S. M. Bilenky, F. Capozzi, and S. T. Petcov, An alternative method of determining the neutrino mass ordering in reactor neutrino experiments, Phys. Lett. B **772**, 179 (2017).

[122] P. F. de Salas, D. V. Forero, C. A. Ternes, M. Tortola, and J. W. F. Valle, Status of neutrino oscillations 2018: 3σ hint for normal mass ordering and improved *CP* sensitivity, Phys. Lett. B **782**, 633 (2018).

[123] S. Hannestad and T. Schwetz, Cosmology and the neutrino mass ordering, J. Cosmol. Astropart. Phys. 11 (2016) 035.

[124] R. Lazkoz, V. Salzano, and I. Sendra, Oscillations in the dark energy EoS: New MCMC lessons, Phys. Lett. B **694**, 198 (2010).

[125] J.-Z. Ma and X. Zhang, Probing the dynamics of dark energy with novel parametrizations, Phys. Lett. B **699**, 233 (2011).

[126] G. Pantazis, S. Nesseris, and L. Perivolaropoulos, Comparison of thawing and freezing dark energy parametrizations, Phys. Rev. D **93**, 103503 (2016).

[127] W. Yang, S. Pan, and A. Paliathanasis, Latest astronomical constraints on some nonlinear parametric dark energy models, Mon. Not. R. Astron. Soc. **475**, 2605 (2018).

[128] R. J. F. Marcondes and S. Pan, Cosmic chronometers constraints on some fast-varying dark energy equations of state, arXiv:1711.06157.

[129] S. Pan, E. N. Saridakis, and W. Yang, Observational constraints on oscillating dark-energy parametrizations, Phys. Rev. D **98**, 063510 (2018).

[130] X. Zhang, Impacts of dark energy on weighing neutrinos after Planck 2015, Phys. Rev. D **93**, 083011 (2016).

[131] S. Wang, Y.-F. Wang, D.-M. Xia, and X. Zhang, Impacts of dark energy on weighing neutrinos: Mass hierarchies considered, Phys. Rev. D **94**, 083519 (2016).

[132] M.-M. Zhao, Y.-H. Li, J.-F. Zhang, and X. Zhang, Constraining neutrino mass and extra relativistic degrees of freedom in dynamical dark energy models using Planck 2015 data in combination with low-redshift cosmological probes: Basic extensions to ΛCDM cosmology, Mon. Not. R. Astron. Soc. **469**, 1713 (2017).

[133] R.-Y. Guo, Y.-H. Li, J.-F. Zhang, and X. Zhang, Weighing neutrinos in the scenario of vacuum energy interacting with cold dark matter: Application of the parameterized post-Friedmann approach, J. Cosmol. Astropart. Phys. 05 (2017) 040.

[134] X. Zhang, Weighing neutrinos in dynamical dark energy models, Sci. China Phys. Mech. Astron. **60**, 060431 (2017).

[135] E.-K. Li, H. Zhang, M. Du, Z.-H. Zhou, and L. Xu, Probing the neutrino mass hierarchy beyond ΛCDM model, J. Cosmol. Astropart. Phys. 08 (2018) 042.
[136] W. Yang, R. C. Nunes, S. Pan, and D. F. Mota, Effects of neutrino mass hierarchies on dynamical dark energy models, Phys. Rev. D **95**, 103522 (2017).
[137] S. Peirone, M. Martinelli, M. Raveri, and A. Silvestri, Impact of theoretical priors in cosmological analyses: The case of single field quintessence, Phys. Rev. D **96**, 063524 (2017).
[138] R.-Y. Guo, J.-F. Zhang, and X. Zhang, Exploring neutrino mass and mass hierarchy in the scenario of vacuum energy interacting with cold dark matter, Chin. Phys. C **42**, 095103 (2018).
[139] N. Aghanim *et al.* (Planck Collaboration), Planck 2015 results. XI. CMB power spectra, likelihoods, and robustness of parameters, Astron. Astrophys. **594**, A11 (2016).
[140] N. Aghanim *et al.* (Planck Collaboration), Planck intermediate results. XLVI. Reduction of large-scale systematic effects in HFI polarization maps and estimation of the reionization optical depth, Astron. Astrophys. **596**, A107 (2016).
[141] L. Anderson *et al.* (BOSS Collaboration), The clustering of galaxies in the SDSS-III Baryon Oscillation Spectroscopic Survey: Baryon acoustic oscillations in the Data Releases 10 and 11 Galaxy samples, Mon. Not. R. Astron. Soc. **441**, 24 (2014).
[142] A. J. Ross, L. Samushia, C. Howlett, W. J. Percival, A. Burden, and M. Manera, The clustering of the SDSS DR7 main Galaxy sample? I. A 4 per cent distance measure at $z = 0.15$, Mon. Not. R. Astron. Soc. **449**, 835 (2015).
[143] F. Beutler, C. Blake, M. Colless, D. Heath Jones, L. Staveley-Smith, L. Campbell, Q. Parker, W. Saunders, and F. Watson, The 6dF Galaxy Survey: Baryon acoustic oscillations and the local Hubble constant, Mon. Not. R. Astron. Soc. **416**, 3017 (2011).
[144] M. Betoule *et al.* (SDSS Collaboration), Improved photometric calibration of the SNLS and the SDSS Supernova Surveys, Astron. Astrophys. **552**, A124 (2013).
[145] M. Betoule *et al.* (SDSS Collaboration), Improved cosmological constraints from a joint analysis of the SDSS-II and SNLS supernova samples, Astron. Astrophys. **568**, A22 (2014).
[146] J. Mosher *et al.*, Cosmological parameter uncertainties from SALT-II Type Ia supernova light curve models, Astrophys. J. **793**, 16 (2014).
[147] A. Lewis and S. Bridle, Cosmological parameters from CMB and other data: A Monte Carlo approach, Phys. Rev. D **66**, 103511 (2002).
[148] M. Gerbino, K. Freese, S. Vagnozzi, M. Lattanzi, O. Mena, E. Giusarma, and S. Ho, Impact of neutrino properties on the estimation of inflationary parameters from current and future observations, Phys. Rev. D **95**, 043512 (2017).
[149] H. Tak, S. K. Ghosh, and J. A. Ellis, How proper are Bayesian models in the astronomical literature?, Mon. Not. R. Astron. Soc. **481**, 277 (2018).
[150] F. Simpson, R. Jimenez, C. Pena-Garay, and L. Verde, Strong Bayesian evidence for the normal neutrino hierarchy, J. Cosmol. Astropart. Phys. 06 (2017) 029.
[151] T. Schwetz *et al.*, Comment on "Strong evidence for the normal neutrino hierarchy", arXiv:1703.04585.
[152] S. Hannestad and T. Tram, Optimal prior for Bayesian inference in a constrained parameter space, arXiv:1710.08899.
[153] A. J. Long, M. Raveri, W. Hu, and S. Dodelson, Neutrino mass priors for cosmology from random matrices, Phys. Rev. D **97**, 043510 (2018).
[154] S. Gariazzo, M. Archidiacono, P. F. de Salas, O. Mena, C. A. Ternes, and M. Tórtola, Neutrino masses and their ordering: Global data, priors and models, J. Cosmol. Astropart. Phys. 03 (2018) 011.
[155] A. F. Heavens and E. Sellentin, Objective Bayesian analysis of neutrino masses and hierarchy, J. Cosmol. Astropart. Phys. 04 (2018) 047.
[156] W. Handley and M. Millea, Maximum entropy priors with derived parameters in a specified distribution, arXiv:1804.08143.
[157] P. F. De Salas, S. Gariazzo, O. Mena, C. A. Ternes, and M. Tórtola, Neutrino mass ordering in 2018: Global status, arXiv:1806.11051.
[158] J. F. Beacom, N. F. Bell, and S. Dodelson, Neutrinoless Universe, Phys. Rev. Lett. **93**, 121302 (2004).
[159] M. Gerbino, M. Lattanzi, O. Mena, and K. Freese, A novel approach to quantifying the sensitivity of current and future cosmological datasets to the neutrino mass ordering through Bayesian hierarchical modeling, Phys. Lett. B **775**, 239 (2017).
[160] C. Heymans *et al.*, CFHTLenS: The Canada-France-Hawaii Telescope Lensing Survey, Mon. Not. R. Astron. Soc. **427**, 146 (2012).
[161] M. Kilbinger *et al.*, CFHTLenS: Combined probe cosmological model comparison using 2D weak gravitational lensing, Mon. Not. R. Astron. Soc. **430**, 2200 (2013).
[162] C. Heymans *et al.*, CFHTLenS tomographic weak lensing cosmological parameter constraints: Mitigating the impact of intrinsic galaxy alignments, Mon. Not. R. Astron. Soc. **432**, 2433 (2013).
[163] E. Macaulay, I. K. Wehus, and H. K. Eriksen, Lower Growth Rate from Recent Redshift Space Distortion Measurements than Expected from Planck, Phys. Rev. Lett. **111**, 161301 (2013).
[164] N. MacCrann, J. Zuntz, S. Bridle, B. Jain, and M. R. Becker, Cosmic discordance: Are Planck CMB and CFHTLenS weak lensing measurements out of tune?, Mon. Not. R. Astron. Soc. **451**, 2877 (2015).
[165] M. Raveri, Are cosmological data sets consistent with each other within the Λ cold dark matter model?, Phys. Rev. D **93**, 043522 (2016).
[166] S. Joudaki *et al.*, CFHTLenS revisited: Assessing concordance with Planck including astrophysical systematics, Mon. Not. R. Astron. Soc. **465**, 2033 (2017).
[167] T. D. Kitching, L. Verde, A. F. Heavens, and R. Jimenez, Discrepancies between CFHTLenS cosmic shear and Planck: New physics or systematic effects?, Mon. Not. R. Astron. Soc. **459**, 971 (2016).
[168] H. Hildebrandt *et al.*, KiDS-450: Cosmological parameter constraints from tomographic weak gravitational lensing, Mon. Not. R. Astron. Soc. **465**, 1454 (2017).

[169] P. Ko and Y. Tang, Light dark photon and fermionic dark radiation for the Hubble constant and the structure formation, Phys. Lett. B **762**, 462 (2016).

[170] A. Leauthaud *et al.*, Lensing is low: Cosmology, galaxy formation, or new physics?, Mon. Not. R. Astron. Soc. **467**, 3024 (2017).

[171] S. Camera, M. Martinelli, and D. Bertacca, Easing tensions with quartessence, arXiv:1704.06277.

[172] E. Di Valentino, C. Bøehm, E. Hivon, and F. R. Bouchet, Reducing the H_0 and σ_8 tensions with dark matter–neutrino interactions, Phys. Rev. D **97**, 043513 (2018).

[173] A. Gomez-Valent and J. Sola, Relaxing the σ_8-tension through running vacuum in the Universe, Europhys. Lett. **120**, 39001 (2017).

[174] A. Gómez-Valent and J. Solà Peracaula, Density perturbations for running vacuum: A successful approach to structure formation and to the σ_8-tension, Mon. Not. R. Astron. Soc. **478**, 126 (2018).

[175] A. G. Riess, L. Macri, S. Casertano, H. Lampeitl, H. C. Ferguson, A. V. Filippenko, S. W. Jha, W. Li, and R. Chornock, A 3% solution: Determination of the hubble constant with the hubble space telescope and wide field camera 3, Astrophys. J. **730**, 119 (2011); Astrophys. J. **732**, 129(E) (2011).

[176] A. G. Riess *et al.*, A 2.4% determination of the local value of the Hubble constant, Astrophys. J. **826**, 56 (2016).

[177] E. Di Valentino, A. Melchiorri, and J. Silk, Beyond six parameters: Extending ΛCDM, Phys. Rev. D **92**, 121302 (2015).

[178] E. Di Valentino, A. Melchiorri, and J. Silk, Reconciling Planck with the local value of H_0 in extended parameter space, Phys. Lett. B **761**, 242 (2016).

[179] J. L. Bernal, L. Verde, and A. G. Riess, The trouble with H_0, J. Cosmol. Astropart. Phys. 10 (2016) 019.

[180] G.-B. Zhao *et al.*, Dynamical dark energy in light of the latest observations, Nat. Astron. **1**, 627 (2017).

[181] E. Di Valentino, Crack in the cosmological paradigm, Nat. Astron. **1**, 569 (2017).

[182] V. Salvatelli, A. Marchini, L. Lopez-Honorez, and O. Mena, New constraints on coupled dark energy from the Planck satellite experiment, Phys. Rev. D **88**, 023531 (2013).

[183] Q.-G. Huang and K. Wang, How the dark energy can reconcile Planck with local determination of the Hubble constant, Eur. Phys. J. C **76**, 506 (2016).

[184] T. Karwal and M. Kamionkowski, Dark energy at early times, the Hubble parameter, and the string axiverse, Phys. Rev. D **94**, 103523 (2016).

[185] S. Kumar and R. C. Nunes, Probing the interaction between dark matter and dark energy in the presence of massive neutrinos, Phys. Rev. D **94**, 123511 (2016).

[186] A. Shafieloo, D. K. Hazra, V. Sahni, and A. A. Starobinsky, Metastable dark energy with radioactive-like decay, Mon. Not. R. Astron. Soc. **473**, 2760 (2018).

[187] S. Kumar and R. C. Nunes, Echo of interactions in the dark sector, Phys. Rev. D **96**, 103511 (2017).

[188] L. Feng, J.-F. Zhang, and X. Zhang, A search for sterile neutrinos with the latest cosmological observations, Eur. Phys. J. C **77**, 418 (2017).

[189] M.-M. Zhao, D.-Z. He, J.-F. Zhang, and X. Zhang, Search for sterile neutrinos in holographic dark energy cosmology: Reconciling Planck observation with the local measurement of the Hubble constant, Phys. Rev. D **96**, 043520 (2017).

[190] E. Di Valentino, A. Melchiorri, E. V. Linder, and J. Silk, Constraining dark energy dynamics in extended parameter space, Phys. Rev. D **96**, 023523 (2017).

[191] E. Di Valentino, A. Melchiorri, and O. Mena, Can interacting dark energy solve the H_0 tension?, Phys. Rev. D **96**, 043503 (2017).

[192] W. Yang, N. Banerjee, and S. Pan, Constraining a dark matter and dark energy interaction scenario with a dynamical equation of state, Phys. Rev. D **95**, 123527 (2017).

[193] L. Feng, J.-F. Zhang, and X. Zhang, Searching for sterile neutrinos in dynamical dark energy cosmologies, Sci. China Phys. Mech. Astron. **61**, 050411 (2018).

[194] W. Yang, S. Pan, and D. F. Mota, Novel approach toward the large-scale stable interacting dark-energy models and their astronomical bounds, Phys. Rev. D **96**, 123508 (2017).

[195] D. Wang and X.-H. Meng, No evidence for dynamical dark energy in two models, Phys. Rev. D **96**, 103516 (2017).

[196] E. Di Valentino, E. V. Linder, and A. Melchiorri, Vacuum phase transition solves the H_0 tension, Phys. Rev. D **97**, 043528 (2018).

[197] S. Pan, A. Mukherjee, and N. Banerjee, Astronomical bounds on a cosmological model allowing a general interaction in the dark sector, Mon. Not. R. Astron. Soc. **477**, 1189 (2018).

[198] L. Feng, J.-F. Zhang, and X. Zhang, Search for sterile neutrinos in a universe of vacuum energy interacting with cold dark matter, arXiv:1712.03148.

[199] J. Matsumoto, Phantom crossing dark energy in Horndeski's theory, Phys. Rev. D **97**, 123538 (2018).

[200] D. Wang, Dark energy constraints in light of Pantheon SNe Ia, BAO, cosmic chronometers and CMB polarization and lensing data, Phys. Rev. D **97**, 123507 (2018).

[201] E. Mörtsell and S. Dhawan, Does the Hubble constant tension call for new physics?, arXiv:1801.07260.

[202] V. Poulin, K. K. Boddy, S. Bird, and M. Kamionkowski, Implications of an extended dark energy cosmology with massive neutrinos for cosmological tensions, Phys. Rev. D **97**, 123504 (2018).

[203] W. Yang, S. Pan, L. Xu, and D. F. Mota, Effects of anisotropic stress in interacting dark matter–dark energy scenarios, arXiv:1804.08455.

[204] W. Yang, S. Pan, E. Di Valentino, R. C. Nunes, S. Vagnozzi, and D. F. Mota, Tale of stable interacting dark energy, observational signatures, and the H_0 tension, J. Cosmol. Astropart. Phys. 09 (**2018**) 019.

[205] E. Di Valentino and L. Mersini-Houghton, Testing predictions of the Quantum Landscape Multiverse 3: The hilltop inflationary potential, arXiv:1807.10833.

[206] W. Yang, S. Pan, R. Herrera, and S. Chakraborty, Large-scale (in) stability analysis of an exactly solved coupled dark-energy model, Phys. Rev. D **98**, 043517 (2018).

[207] J. Sola, Cosmological constant and vacuum energy: Old and new ideas, J. Phys. Conf. Ser. **453**, 012015 (2013).

[208] J. Sola, A. Gomez-Valent, and J. de Cruz Pérez, Hints of dynamical vacuum energy in the expanding Universe, Astrophys. J. **811**, L14 (2015).

[209] J. Solà, A. Gómez-Valent, and J. de Cruz Pérez, First evidence of running cosmic vacuum: Challenging the concordance model, Astrophys. J. **836**, 43 (2017).

[210] J. Solà Peracaula, J. de Cruz Pérez, and A. Gómez-Valent, Dynamical dark energy vs $\Lambda = \text{const}$ in light of observations, Europhys. Lett. **121**, 39001 (2018).

[211] J. Solà, Cosmological constant vis-a-vis dynamical vacuum: Bold challenging the ΛCDM, Int. J. Mod. Phys. A **31**, 1630035 (2016).

[212] J. Sola, A. Gomez-Valent, and J. de Cruz Pérez, Dynamical dark energy: Scalar fields and running vacuum, Mod. Phys. Lett. A **32**, 1750054 (2017).

[213] J. Solà Peracaula, J. d. C. Perez, and A. Gomez-Valent, Possible signals of vacuum dynamics in the Universe, Mon. Not. R. Astron. Soc. **478**, 4357 (2018).

[214] J. Solà, A. Gómez-Valent, and J. de Cruz Pérez, The H_0 tension in light of vacuum dynamics in the Universe, Phys. Lett. B **774**, 317 (2017).

[215] J. Solà, A. Gómez-Valent, and J. de Cruz Pérez, Vacuum dynamics in the Universe versus a rigid $\Lambda = \text{const}$, Int. J. Mod. Phys. A **32**, 1730014 (2017).

[216] V. Sahni, A. Shafieloo, and A. A. Starobinsky, Two new diagnostics of dark energy, Phys. Rev. D **78**, 103502 (2008).

[217] R. Trotta, Bayes in the sky: Bayesian inference and model selection in cosmology, Contemp. Phys. **49**, 71 (2008).

[218] L. Verde, Statistical methods in cosmology, Lect. Notes Phys. **800**, 147 (2010).

[219] K. Abe *et al.* (T2K Collaboration), The T2K Experiment, Nucl. Instrum. Methods Phys. Res., Sect. A **659**, 106 (2011).

[220] R. B. Patterson (NOvA Collaboration), The NOvA Experiment: Status and outlook, Nucl. Phys. B, Proc. Suppl. **235–236**, 151 (2013).

[221] R. Acciarri *et al.* (DUNE Collaboration), Long-Baseline Neutrino Facility (LBNF) and Deep Underground Neutrino Experiment (DUNE), arXiv:1512.06148.

[222] R. Fardon, A. E. Nelson, and N. Weiner, Dark energy from mass varying neutrinos, J. Cosmol. Astropart. Phys. 10 (2004) 005.

[223] U. Franca, M. Lattanzi, J. Lesgourgues, and S. Pastor, Model independent constraints on mass-varying neutrino scenarios, Phys. Rev. D **80**, 083506 (2009).

[224] C. Wetterich, Variable gravity Universe, Phys. Rev. D **89**, 024005 (2014).

[225] C.-Q. Geng, C.-C. Lee, R. Myrzakulov, M. Sami, and E. N. Saridakis, Observational constraints on varying neutrino-mass cosmology, J. Cosmol. Astropart. Phys. 01 (2016) 049.

[226] L. Knox, Y.-S. Song, and J. A. Tyson, Distance-redshift and growth-redshift relations as two windows on acceleration and gravitation: Dark energy or new gravity?, Phys. Rev. D **74**, 023512 (2006).

[227] D. Huterer and E. V. Linder, Separating dark physics from physical darkness: Minimalist modified gravity vs dark energy, Phys. Rev. D **75**, 023519 (2007).

[228] M. Kunz and D. Sapone, Dark Energy versus Modified Gravity, Phys. Rev. Lett. **98**, 121301 (2007).

[229] B. Hu, M. Raveri, A. Silvestri, and N. Frusciante, Exploring massive neutrinos in dark cosmologies with EFTCAMB/ EFTCosmoMC, Phys. Rev. D **91**, 063524 (2015).

[230] R. A. Battye, B. Bolliet, and J. A. Pearson, $f(R)$ gravity as a dark energy fluid, Phys. Rev. D **93**, 044026 (2016).

[231] N. Bellomo, E. Bellini, B. Hu, R. Jimenez, C. Pena-Garay, and L. Verde, Hiding neutrino mass in modified gravity cosmologies, J. Cosmol. Astropart. Phys. 02 (2017) 043.

[232] Y. Dirian, Changing the Bayesian prior: Absolute neutrino mass constraints in nonlocal gravity, Phys. Rev. D **96**, 083513 (2017).

[233] J. Renk, M. Zumalacárregui, F. Montanari, and A. Barreira, Galileon gravity in light of ISW, CMB, BAO and H_0 data, J. Cosmol. Astropart. Phys. 10 (**2017**) 020.

[234] S. Peirone, N. Frusciante, B. Hu, M. Raveri, and A. Silvestri, Do current cosmological observations rule out all covariant Galileons?, Phys. Rev. D **97**, 063518 (2018).

[235] C. Vafa, The string landscape and the swampland, arXiv:hep-th/0509212.

[236] G. Obied, H. Ooguri, L. Spodyneiko, and C. Vafa, De Sitter space and the swampland, arXiv:1806.08362.

[237] P. Agrawal, G. Obied, P. J. Steinhardt, and C. Vafa, On the cosmological implications of the string swampland, Phys. Lett. B **784**, 271 (2018).

[238] D. Andriot, On the de Sitter swampland criterion, arXiv:1806.10999.

[239] G. Dvali and C. Gomez, On exclusion of positive cosmological constant, arXiv:1806.10877.

[240] A. Achúcarro and G. A. Palma, The string swampland constraints require multi-field inflation, arXiv:1807.04390.

[241] S. K. Garg and C. Krishnan, Bounds on slow roll and the de Sitter swampland, arXiv:1807.05193.

[242] A. Kehagias and A. Riotto, A note on inflation and the swampland, arXiv:1807.05445.

[243] C.-I. Chiang and H. Murayama, Building supergravity quintessence model, arXiv:1808.02279.

[244] L. Heisenberg, M. Bartelmann, R. Brandenberger, and A. Refregier, Dark energy in the swampland, arXiv:1808.02877.

[245] W. H. Kinney, S. Vagnozzi, and L. Visinelli, The zoo plot meets the swampland: Mutual (in)consistency of single-field inflation, string conjectures, and cosmological data, arXiv:1808.06424.

[246] M. Cicoli, S. De Alwis, A. Maharana, F. Muia, and F. Quevedo, De Sitter vs quintessence in string theory, arXiv:1808.08967.

[247] S. Kachru and S. Trivedi, A comment on effective field theories of flux vacua, arXiv:1808.08971.

[248] Y. Akrami, R. Kallosh, A. Linde, and V. Vardanyan, The landscape, the swampland and the era of precision cosmology, arXiv:1808.09440.
[249] M. C. D. Marsh, The swampland, quintessence and the vacuum energy, arXiv:1809.00726.
[250] U. H. Danielsson, The quantum swampland, arXiv:1809.04512.
[251] J.-B. Durrive, J. Ooba, K. Ichiki, and N. Sugiyama, Updated observational constraints on quintessence dark energy models, Phys. Rev. D **97**, 043503 (2018).
[252] H. Akaike, A new look at the statistical model identification, IEEE Trans. Autom. Control **19**, 716 (1974).
[253] R. E. Kass and A. E. Raftery, Bayes factors, J. Am. Stat. Assoc. **90**, 773 (1995).